الجمهورية الجزائرية الديمقراطية الشعبية

PEOPLE'S DEMOCRATIC REPUBLIC OF ALGERIA

وزارة التعليم العالي و البحث العلمي

MINISTRY OF HIGHER EDUCATION AND SCIENTIFIC RESEARCH

جامعة عباس لغرور خنشلة

ABBES LAGHROUR - KHENCHELA UNIVERSITY

Faculty of Sciences and Technology — كلية العلوم والتكنولوجيا

Department of Mathematics — قسم الرياضيات

Serial number: ……………

THESIS

Submitted in Partial Execution of the Requirements of the Degree of

DOCTORATE IN MATHEMATICS

In the field of: ***Mathematics***

Option: ***Applied Mathematics***

Titled by:

Carleman Inequalities for singular Parabolic Equations and Applications

Submitted by: **Nedjma Mahdi**

Directed by : **Ramoul Hichem**

Assessment committee

Saoudi Khaled	Prof	*Khenchela University*	President
Ramoul Hichem	MCA	*Khenchela University*	Supervisor
Kouachi Said	Prof Emeritus	*Khenchela University*	Examiner
Aouafi Rabia	MCA	*Khenchela University*	Examiner
Imad Rezzoug	Prof	*Oum El Bouaghi University*	Examiner
Oussaeif Taki Eddine	Prof	*Oum El Bouaghi University*	Examiner

Academic year: 2025-2026

بسم الله الرحمن الرحيم

Dedication

I dedicate this thesis first and foremost to my beloved family.

To my father, I express my deepest gratitude for his constant support, patience, and encouragement throughout my academic journey. To the memory of my dear mother, whose love, values, and prayers continue to guide me every day; her presence remains deeply rooted in every step of my life.

I dedicate this work to my wife, whose patience, understanding, and quiet strength have sustained me. Her sacrifices and steady encouragement gave meaning to every long night, and difficult day.. Without her support, this work would never have reached its end.

To my daughter and my three sons, I offer this thesis with deep love. You have been my daily reminder of purpose and hope—the reason I kept moving forward, even when the road felt heavy. Your laughter and trust have been my best reward, if anything.

I also dedicate these pages to my brothers and sisters, whose affection and moral support have been constant. Their words, simple yet sincere, often brought the balance I needed in moments of doubt.

This thesis is equally dedicated to all my colleagues at Athmany Abdelmadjid High School. Working beside such devoted educators has been a privilege; your cooperation and commitment have shaped my own sense of perseverance and duty.

Lastly, I wish to express my gratitude to the teachers and colleagues of the Mathematics Laboratory. Their advice, discussions, and steady encouragement have guided me more than words can say... This work carries their influence in every line.

Acknowledgement

I wish to express my heartfelt gratitude to all those who, in one way or another, helped bring this doctoral work to its completion. Their presence, advice, and encouragement have marked every stage of this long journey..

Before anyone else, I owe my deepest thanks to my supervisor, **Dr. Ramoul Hichem (MCA, Khenchela University)**, for his patient guidance and constant support. His scientific discipline, clarity of thought, and encouragement were decisive in shaping this thesis; I am truly indebted for the time and care he devoted to this work.

My sincere appreciation also goes to **Professor Saoudi Khaled (Khenchela University)**, who kindly accepted to chair the assessment committee. His attention and interest in my research are deeply valued — and I am honored by his presence.

I am equally grateful to **Professor Kouachi Said (Professor Emeritus, Khenchela University)** for agreeing to examine this thesis. His insightful comments and kind participation bring great value to this work, and I thank him sincerely for his generosity and availability.

Warm thanks are due to **Dr. Aouafi Rabia (MCA, Khenchela University)** for accepting to examine the manuscript and for her careful reading, constructive remarks, and professional insight. (she read with such care, it felt as though each line mattered...)

I also extend my gratitude to **Professor Imad Rezzoug (Oum El Bouaghi University)** and **Professor Oussaeif Taki Eddine (Oum El Bouaghi University)** for their participation as jury members. Their remarks and expertise are greatly appreciated, of course.

My acknowledgment extends as well to all my colleagues and teachers of the **Department of Mathematics and Computer Science** and the **Mathematics Laboratory at Abbes Laghrour University of Khenchela**. Their discussions, cooperation, and daily scientific exchange have created a motivating environment that enriched this research...

I also wish to pay tribute to the memory of **Professor Adjrode**, whose devotion to teaching and research continues to inspire those who had the

honor to work with him.

To all who, in whatever form, contributed to this work — academically, professionally, or personally — I express my sincere gratitude and respect.

الملخص

تتناول هذه الأطروحة دراسة **مسائل عكسية لتحديد المصدر** في **معادلات قطع مكافئة شاذة ومتدهورة،** بما في ذلك **نماذج الانتشار ذات المشتقات الكسرية في الزمن** .

تظهر هذه المسائل في العديد من التطبيقات العلمية، غير أنها تُعد بطبيعتها **غير حسنة الوضع،** وذلك بسبب التأثيرات التنعيمية الملازمة لظواهرا لإنتشار، إضافة إلى وجود **جهود شاذة من النوع العكسي التربيعي،** مما يؤدي إلى فقدان الإهليلجية للمؤثر التفاضلي.

في الجزء الأول، تعتمد الأطروحة مقاربة **التحكم الأمثل** لمعالجة مسائل تحديد المصدر. حيث يُنظر إلى المصدر المجهول على أنه **متغير تحكم،** ويتم تحديده باعتباره **المقلِّل** لدالة **كلفة** تعتمد على ملاحظات عند الزمن النهائي. وتحت فرضيات مناسبة على معامل الشذوذ، يتم إثبات **حسن وضع** المسألة المباشرة في **فضاءات سوبوليف الموزونة،** كما يُبرهن على وجود حلول أمثلية، ويتم استخلاص **تقديرات استقرارية** للمسألة العكسية. إضافة إلى ذلك، يتم اقتراح طرق **إعادة بناء عددية** تعتمد على خوارزميات تكرارية ، ويتم التحقق من فعاليتها من خلال تجارب عددية.

بعد ذلك، تُوسَّع الدراسة لتشمل **معادلات الانتشار الكسرية في الزمن** ذات **الجهد الشاذ العكسي التربيع** وفي هذا الإطار، تؤدي الطبيعة **غير المحلية** للمشتقات الكسرية في الزمن إلى صعوبات إضافية على المستويين التحليلي والعددي. ومع ذلك، يتم التوصل إلى نتائج **وحدانية** لمسألة تحديد المصدر العكسي، كما تُبرز المحاكاة العددية تأثير رتبة الاشتقاق الكسري ومستوى الضجيج على جودة عملية إعادة البناء.

أما الجزء الأخير من الأطروحة، فقد خُصص لدراسة **متباينات كارلمان** لمؤثرات قطع مكافئة شاذة. حيث تم تطوير إطار تحليلي يعتمد على **أوزان كارلمان المزاحة،** الملائمة لمؤثرات تحتوي على شذوذ داخلي من النوع العكسي التربيعي، وتم الحصول على عدة **تقديرات وسطية** أساسية. وعلى الرغم من أن **متباينة كارلمان العامة** لم تُستكمل بعد، إلا أن البنية العامة للتقدير قد تم تحديدها بوضوح، كما تم تحليل **الصعوبات التحليلية** الرئيسية بدقة، ولا سيما تلك المرتبطة بـ **حجج التمركز** و**متباينات كاتشيوبولي** في وجود أوزان شاذة. ويُعد هذا العمل أساسًا متينًا لأبحاث جارية تُنجز بالتعاون مع المشرف على الأطروحة

بصفة عامة، تقدم هذه الأطروحة إسهامات نظرية وعددية في تحليل المسائل العكسية المرتبطة بمعادلات قطع مكافئة شاذة وكسرية، مع إبراز عدة آفاق بحثية مفتوحة.

الكلمات المفتاحية: مسائل عكسية, معادلات قطع مكافئة شاذة, المشتقات الكسرية في الزمن, التحكم الأمثل, متباينات كارلمان, متباينات كاتشيوبولي, إعادة البناء العددي.

.

Abstract

This thesis is devoted to the study of inverse source problems for singular and degenerate parabolic equations, including time-fractional diffusion models. Such problems arise naturally in many applications, but they are intrinsically ill-posed due to the smoothing effects of diffusion and, in the present setting, the presence of inverse-square singular potentials. These singularities destroy uniform ellipticity and require refined analytical tools to recover stability and uniqueness.

The first part of the thesis adopts an optimal control perspective to address inverse source identification problems. The unknown source is treated as a control variable and recovered as the minimizer of a suitable cost functional involving final-time observations. Under subcritical assumptions on the singular potential, we establish the well-posedness of the direct problem in appropriate weighted Sobolev spaces, prove the existence of optimal controls, and derive stability estimates for the inverse problem. Numerical reconstruction algorithms based on iterative regularization methods are proposed and validated through computational experiments.

The analysis is then extended to time-fractional diffusion equations with inverse-square potentials. In this setting, the nonlocal nature of fractional time derivatives introduces additional analytical and numerical challenges. Nevertheless, uniqueness results for the inverse source problem are obtained, and numerical simulations illustrate the influence of the fractional order and noise on the reconstruction process.

The final part of the thesis is devoted to the study of Carleman inequalities for singular parabolic operators. We develop a shifted Carleman framework adapted to operators with interior inverse-square singularities and establish several key intermediate estimates. While the complete global Carleman inequality is not yet achieved, the analytical structure is clearly identified, and the main technical difficulties—particularly those related to localization arguments and Caccioppoli-type inequalities with singular weights—are thoroughly analyzed. This work lays the foundation for ongoing research conducted in collaboration with the supervisor.

Overall, this thesis contributes to the theoretical and numerical analysis of inverse problems for singular and fractional parabolic equations and highlights several challenging directions for future investigation.

Keywords: inverse problem, singular and degenerate parabolic equation, diffusion, optimal control, stability, numerical reconstruction.

Résumé

Cette thèse est consacrée à l'étude de problèmes inverses de source pour des équations paraboliques singulières et dégénérées, incluant des modèles de diffusion à dérivée fractionnaire en temps. De tels problèmes apparaissent naturellement dans de nombreuses applications scientifiques, mais ils sont intrinsèquement mal posés, en raison à la fois des effets de régularisation propres aux phénomènes de diffusion et de la présence de potentiels singuliers de type inverse-carré, qui entraînent une perte d'ellipticité de l'opérateur.

Dans une première partie, la thèse adopte un point de vue de contrôle optimal pour traiter les problèmes d'identification de source. La source inconnue est considérée comme une variable de contrôle et est déterminée comme le minimiseur d'une fonctionnelle de coût basée sur des observations à temps final. Sous des hypothèses de sous-criticité appropriées sur le paramètre singulier, on établit le caractère bien posé du problème direct dans des espaces de Sobolev pondérés, on démontre l'existence de solutions optimales et on dérive des estimations de stabilité pour le problème inverse. Des méthodes de reconstruction numérique, fondées sur des algorithmes itératifs de régularisation, sont proposées et validées par des expériences numériques.

L'analyse est ensuite étendue aux équations de diffusion fractionnaire en temps comportant un potentiel singulier inverse-carré. Dans ce cadre, la nature non locale des dérivées fractionnaires en temps engendre des difficultés supplémentaires, tant sur le plan analytique que numérique. Néanmoins, des résultats d'unicité pour le problème inverse de source sont obtenus, et des simulations numériques mettent en évidence l'influence de l'ordre fractionnaire et du bruit sur la qualité de la reconstruction.

La dernière partie de la thèse est consacrée à l'étude des inégalités de Carleman pour des opérateurs paraboliques singuliers. Un cadre analytique fondé sur des poids de Carleman décalés est développé pour des opérateurs présentant des singularités intérieures de type inverse-carré, et plusieurs estimations intermédiaires essentielles sont établies. Bien que l'inégalité de Carleman globale complète ne soit pas encore entièrement obtenue, la structure de l'estimation est clairement identifiée et les principales difficultés analytiques — notamment celles liées aux arguments de localisation et aux inégalités de Caccioppoli en présence de poids singuliers — sont analysées en détail. Ce travail constitue une base solide pour des recherches en cours menées en collaboration avec le directeur de thèse.

Dans son ensemble, cette thèse apporte des contributions théoriques et numériques à l'analyse des problèmes inverses pour des équations paraboliques singulières et fractionnaires, tout en mettant en évidence plusieurs perspectives de recherche ouvertes

Mots-clés : problème inverse, équation parabolique singulière et dégénérée, diffusion, contrôle optimal, stabilité, reconstruction numérique.

Contents

List of Figures

List of Tables

Abreviations list

Acronyme	Signification
$\mathbb{R}$	Set of real numbers.
$\mathbb{N}^*$	Set of strictly positive integers.
H	Hilbert space.
$\Omega \subset \mathbb{R}^N$	Bounded open spatial domain.
$\overline{\Omega}$	Closure of the domain Ω.
$\partial\Omega$	Boundary of the domain Ω.
$\vec{n}$	Outward unit normal vector to $\partial\Omega$.
$T > 0$	Final observation time.
$\overline{f}$	Optimal solution of the inverse problem.
PDE	Partial Differential Equation.
s.p	Scalar product.
a.e.	Almost everywhere.
L.F.	Linear form.
U_{ex}	Exact (reference) solution.
U_{inv}	Solution reconstructed by the inverse method.
U_{New}	Solution reconstructed by the Newton method.
U_{ef}	Solution reconstructed by the finite element–Newton method.
$Er.ab$	Absolute error.
$\|Er_{inv}\| = \|U_{ex} - U_{inv}\|_\infty$	Absolute reconstruction error (inverse method).
$\|Er_{New}\| = \|U_{ex} - U_{New}\|_\infty$	Absolute reconstruction error (Newton method).
$\|Er_{ef}\| = \|U_{ex} - U_{ef}\|_\infty$	Absolute reconstruction error (finite element–Newton method).
$\lvert f(x) - f^k(x)\rvert$	Absolute error of the source term f at iteration k.
k	Iteration index.
u^*	Exact solution.
u_f^{365}	Identified solution after 365 iterations.
$\lvert u(x,t) - u_f^{365}(x,t)\rvert$	Absolute error of the solution after 365 iterations.
$\lvert f(x) - f^{365}(x)\rvert$	Absolute error of the source term after 365 iterations.

Acronyme	Signification
K, H	Linear operators.
max	Maximum.
min	Minimum.
sup	Upper bound (supremum).
inf	Lower bound (infimum).
lim	Limit.
$\mathcal{A}$	Admissible set.
$f_{\min}$	Lower bound for the unknown source term $f(x)$.
$f_{\max}$	Upper bound for the unknown source term $f(x)$.
$\lambda > 0$	Regularization parameter.
P	Differential operator defining the state equation.
P^*	Adjoint operator of P.
$\\| \cdot \\|_{L^2}$	Norm of the space L^2.
∇	Gradient operator.
Δ	Laplace operator.
i.e.	That is (id est).
$\\|u\\|^2_{L^2(0,1)}$	$\int_0^1 u(x)^2 \, \mathrm{d}x$.
$(\cdot, \cdot)$	Scalar product.

Standardized Trilingual Terminology Table

English – Français – العربية

English	Français	العربية
Inverse problem	Problème inverse	مسألة عكسية
Direct problem	Problème direct	مسألة مباشرة
Ill-posed problem	Problème mal posé	مسألة غير حسنة الوضع
Well-posedness	Bonne position	حسن الوضع
Existence of solution	Existence de solution	وجود الحل
Uniqueness	Unicité	الوحيدية
Stability	Stabilité	الاستقرارية
Parabolic equation	Équation parabolique	معادلة قطع مكافئة
Singular parabolic equation	Équation parabolique singulière	معادلة قطع مكافئة شاذة
Degenerate equation	Équation dégénérée	معادلة متدهورة
Diffusion equation	Équation de diffusion	معادلة انتشار
Fractional diffusion equation	Équation de diffusion fractionnaire	معادلة انتشار كسرية
Fractional time derivative	Dérivée fractionnaire en temps	مشتقة كسرية في الزمن
Nonlocal operator	Opérateur non local	مؤثر غير محلي
Source term	Terme source	حدّ المصدر
Inverse source problem	Problème inverse de source	مسألة تحديد المصدر العكسي
Source identification	Identification de la source	تحديد المصدر
Final-time observation	Observation à temps final	ملاحظة عند الزمن النهائي
Observation data	Données d'observation	معطيات الرصد
Measurement noise	Bruit de mesure	ضجيج القياس
Optimal control	Contrôle optimal	التحكم الأمثل
Control variable	Variable de contrôle	متغير التحكم
Admissible set	Ensemble admissible	المجموعة المقبولة
Cost functional	Fonctionnelle de coût	دالة الكلفة
Minimizer	Minimiseur	المقلِّل
Regularization	Régularisation	التنظيم
Iterative regularization	Régularisation itérative	تنظيم تكراري
Landweber iteration	Méthode de Landweber	طريقة لاندويبر

English	**Français**	**العربية**
Numerical reconstruction	Reconstruction numérique	إعادة البناء العددية
Numerical simulation	Simulation numérique	محاكاة عددية
Sobolev space	Espace de Sobolev	فضاء سوبوليف
Weighted Sobolev space	Espace de Sobolev pondéré	فضاء سوبوليف موزون
Hardy inequality	Inégalité de Hardy	متباينة هاردي
Singular potential	Potentiel singulier	جهد شاذ
Inverse-square potential	Potentiel inverse-carré	جهد عكسي تربيعي
Subcritical condition	Condition sous-critique	شرط دون-حرج
Ellipticity	Ellipticité	الإهليلجية
Loss of ellipticity	Perte d'ellipticité	فقدان الإهليلجية
Carleman inequality	Inégalité de Carleman	متباينة كارلمان
Carleman estimate	Estimation de Carleman	تقدير كارلمان
Carleman weight	Poids de Carleman	وزن كارلمان
Shifted weight	Poids décalé	وزن مزاح
Conjugation of operator	Conjugaison de l'opérateur	اقتران المؤثر
Conjugated operator	Opérateur conjugué	المؤثر المقترن
Symmetric part	Partie symétrique	الجزء المتماثل
Antisymmetric part	Partie antisymétrique	الجزء غير المتماثل
Interaction term	Terme d'interaction	حد التفاعل
Coercive term	Terme coercif	حد قسري
Localization argument	Argument de localisation	حجة التمركز
Cut-off function	Fonction de coupure	دالة قطع
Caccioppoli inequality	Inégalité de Caccioppoli	متباينة كاتشيوبولي
Time-derivative term	Terme de dérivée temporelle	حد مشتقة زمنية
Singular weight	Poids singulier	وزن شاذ

Chapter 1

Background, Motivation, and Mathematical Framework

Introduction

Inverse problems have gained increasing attention over the past few decades, both for their mathematical depth and for their wide field of applications—in physics, engineering, biology, and geophysics alike. In essence, an inverse problem seeks to determine hidden causes, such as coefficients, source terms, or initial states, from limited or indirect observations of a system's response. This view stands in contrast with direct problems, where one predicts the evolution of a system from complete and known data.

Historically, the first inverse problems grew out of practical needs long before a formal theory existed. Classic examples include determining underground structures from surface data, identifying heat sources from measured temperatures, or reconstructing material properties from experimental readings. Such questions led naturally to mathematical models governed by partial differential equations, where the unknown element appears as a coefficient or forcing term...

The key challenge of these problems lies in their intrinsic ill-posedness in the sense of Hadamard. Unlike direct problems, inverse problems often fail to ensure existence, uniqueness, or stability of solutions. Even in cases where uniqueness holds, the dependence on measured data is notoriously unstable—tiny errors may cause huge deviations in the reconstruction. This instability is not an accident of modelling but an essential structural feature of inverse problems themselves.

Parabolic equations, describing diffusion phenomena, offer a vivid example. Diffusion smooths out spatial variations over time, erasing information about the initial state or internal sources. To reconstruct such data from final-time measurements is therefore to reverse an inherently irreversible process—one of the reasons inverse problems for parabolic equations are among the most delicate.

The modern analytical theory took shape during the latter half of the twentieth century, marked by the introduction of Carleman inequalities. Originally designed for unique–continuation questions, these weighted energy estimates soon proved vital for proving uniqueness and stability in inverse problems. Early works showed that Carleman estimates could recover unknown coefficients or sources in parabolic equations under appropriate observation conditions. Later contributions refined the argument, uncovering deep connections between inverse problems, observability inequalities, and controllability.

When singular or degenerate terms appear in the governing equations, the analysis becomes far more intricate. The inverse–square potential provides a typical case—it arises in quantum mechanics and combustion theory, is critical under scaling, and breaks the uniform ellipticity of the operator. Here Hardy–type inequalities are indispensable for restoring coercivity within the subcritical regime.

In more recent years, fractional diffusion equations have emerged as models for anomalous diffusion, replacing the classical first–order derivative in time by a fractional one to capture memory effects. While physically more accurate, these models bring additional mathematical and numerical difficulty due to the nonlocal nature of the fractional derivative—especially when coupled with singular spatial operators.

The present thesis focuses on inverse source problems for singular and degenerate parabolic equations, including time–fractional models with inverse–square potentials. Instead of attacking the inverse problem directly, it adopts an optimisation–based perspective where the unknown source acts as a control variable, minimising a cost functional that measures the mismatch between observations and model predictions. This formulation naturally introduces regularisation and allows stability results to be derived in a unified manner.

The theoretical developments are accompanied by numerical tests—not only to illustrate but to validate the analysis and to examine reconstruction behaviour under noisy conditions...

The thesis is structured as follows. **Chapter 1** outlines the necessary background: functional analysis, Hardy inequalities, fractional calculus, optimisation, and controllability concepts. **Chapter 2** studies an inverse source problem for a singular parabolic equation through an optimal–control formulation, proving stability and presenting numerical reconstructions. **Chapter**

3 extends the analysis to time–fractional diffusion with inverse–square potentials, addressing uniqueness and numerical identification of sources. **Chapter 4** develops the Carleman framework for singular parabolic operators, identifies the principal analytical difficulties, and sets the groundwork for continuing research. The thesis concludes with a synthesis of the results—and perspectives for what is still to come.

The State of the Art: Functional Analysis, Optimization, Numerical Identification, and Controllability

1.1 Introduction

The study of inverse problems has become a central theme in applied mathematics over the last four decades. Broadly speaking, an inverse problem seeks to identify unknown causes from observed effects. By contrast, a *direct problem* starts with known parameters (coefficients, sources, boundary and initial conditions) and computes the system's response. Inverse problems appear in many applied sciences, including geophysics, tomography, electrocardiology, population dynamics, and heat conduction [18, 43].

The key challenge is that inverse problems are often *ill-posed* in the sense of Hadamard: the solution may fail to exist, may not be unique, or may not depend continuously on the data. This ill-posedness manifests in strong sensitivity to measurement errors. Consequently, solving inverse problems requires combining tools from functional analysis, regularization theory, optimization methods, and control theory.

In the specific case of *singular or degenerate parabolic equations*, the presence of singular potentials (e.g., inverse-square potentials) or degenerate diffusion coefficients adds further complexity. Such models arise in quantum mechanics, combustion theory, anomalous diffusion, and heterogeneous media [7, 6]. They present both analytical challenges, due to the singular structure, and numerical challenges, due to ill-posedness.

This chapter presents a survey of the state of the art in functional analysis, optimization, numerical identification, and controllability as they relate to inverse problems governed by singular or degenerate equations. The structure is as follows. Section 2 reviews the functional analytic framework:

Lebesgue and Sobolev spaces, weighted spaces, and Hardy inequalities. Section 3 recalls basic notions of fractional calculus and singular parabolic operators. Section 4 presents the optimization approach to inverse problems and adjoint-based variational formulations. Section 5 is devoted to numerical reconstruction algorithms, with emphasis on Landweber iteration and the Conjugate Gradient Method (CGM). Section 6 addresses controllability, highlighting Carleman estimates, observability inequalities, and null controllability of singular/degenerate parabolic equations. The chapter closes with a conclusion situating the thesis within this broader context.

1.2 Functional Analysis Background

1.2.1 Lebesgue and Sobolev Spaces

The foundation of modern PDE theory rests on Lebesgue and Sobolev spaces. Lebesgue spaces $L^p(\Omega)$ provide a natural framework for integrability, while Sobolev spaces $H^m(\Omega)$ encode differentiability in the weak sense. These spaces allow one to define weak solutions to PDEs and exploit compactness and interpolation properties.

Sobolev embeddings play a crucial role: $H^1(\Omega)$ is continuously embedded into $L^q(\Omega)$ for suitable q, ensuring that weak solutions of PDEs possess sufficient regularity for physical interpretation. For inverse problems, these embeddings help control stability estimates in reconstruction.

1.2.2 Weighted Sobolev Spaces and Hardy Inequalities

In the presence of singular potentials such as $\mu|x|^{-2}$, standard Sobolev spaces are insufficient. One instead works with weighted Sobolev spaces $H^1_{\mu,0}(\Omega)$ defined by

$$H^1_{\mu,0}(\Omega) = \Big\{u \in H^1_0(\Omega) : \int_\Omega \Big(|u'(x)|^2 - \frac{\mu}{x^2}|u(x)|^2\Big)\, dx < \infty\Big\}.$$

The cornerstone is the Hardy inequality, which in one dimension reads There exists a constant

$C_H > 0$

such that for all $u \in H^1_0(\Omega)$, the Hardy inequality holds

$$\int_\Omega \frac{|u(x)|^2}{x^2}\, dx \le C_H \int_\Omega |u'(x)|^2\, dx, .$$

This inequality ensures coercivity of bilinear forms associated with singular operators and was instrumental in the seminal work of Baras and Goldstein [7]. Later refinements extended these results to higher dimensions and more general potentials [6]. When the singular parameter reaches the critical Hardy constant, coercivity is lost and classical well-posedness results no longer apply.

1.2.3 Compactness and Convergence

Compactness arguments are central in establishing existence and uniqueness of weak solutions. The Rellich–Kondrachov theorem guarantees that bounded sequences in $H^1(\Omega)$ are precompact in $L^2(\Omega)$. For weighted Sobolev spaces, analogous results hold under Hardy-type inequalities. These compactness tools form the basis of many stability proofs in inverse problems.

1.3 Fractional Calculus and Singular Operators

Fractional derivatives are introduced to model memory effects and anomalous diffusion phenomena that cannot be captured by classical parabolic equations

1.3.1 Fractional Derivatives

Fractional calculus generalizes differentiation and integration to non-integer orders. The most widely used definitions are the Riemann–Liouville and Caputo derivatives. For $0 < \alpha < 1$, the Caputo derivative is

$$\partial_t^\alpha u(t) = \frac{1}{\Gamma(1-\alpha)} \int_0^t \frac{u'(s)}{(t-s)^\alpha}\, ds.$$

The Caputo derivative is preferable in modeling since it allows the use of classical initial conditions. Fractional diffusion models capture anomalous diffusion, viscoelasticity, and memory effects [44].

1.3.2 Singular Parabolic Operators

Singular parabolic operators combine classical diffusion with inverse-square potentials:

$$\mathcal{L}_\mu u = -\Delta u - \frac{\mu}{|x|^2} u.$$

For $\mu < \mu^*$, the operator is self-adjoint and generates a contraction semigroup. These operators are central in quantum mechanics (Schrödinger operators with singular potentials) and in diffusion processes in heterogeneous media [7].

1.4 Optimization and Variational Framework

1.4.1 Inverse Problems as Optimization

Many inverse problems are reformulated as optimization problems. A typical cost functional is

$$J(f) = \frac{1}{2}\|u(f)(\cdot, T) - \omega^\delta\|^2_{L^2(\Omega)} + \frac{\gamma}{2}\|f\|^2_{L^2(\Omega)},$$

where $u(f)$ is the solution of the forward problem with source f, ω^δ are noisy data, and $\gamma > 0$ is a regularization parameter. This Tikhonov functional balances fidelity to data with regularity of the solution [18, 43].

1.4.2 Adjoint Equations and Gradient Computation

The gradient of J is computed using adjoint states. If u solves the forward equation and ψ the adjoint backward equation, then

$$J'(f) = \int_0^T \psi(x, t)\, dt.$$

This variational method enables efficient computation of gradients and forms the basis of gradient descent, Landweber iteration, and CGM.

1.4.3 Regularization Methods

Regularization is essential for stabilizing inverse problems. Besides Tikhonov, iterative regularization methods such as Landweber and CGM are widely used. Other approaches include Bayesian inference and variational inequalities [18].

1.5 Numerical Identification

Due to the ill-posed nature of inverse problems, these numerical methods must be coupled with appropriate regularization strategies.

1.5.1 Landweber Iteration

The Landweber iteration is an iterative regularization method that updates the source as

$$f^{k+1} = f^k - \tau J'(f^k).$$

It is simple, robust, and converges for sufficiently small step size τ. However, convergence is slow.

Algorithm 1 Landweber Iteration

```
Initialize f^0 (e.g., f^0 = 0).
for k = 0, 1, 2, ... until stopping criterion do
    Solve forward problem to obtain u(f^k).
    Compute residual r^k = u(f^k)(·, T) − ω^δ.
    Solve adjoint problem with final condition r^k.
    Update f^{k+1} = f^k − τ J'(f^k).
end for
```

Stopping is determined by the discrepancy principle: stop when the data misfit matches the noise level.

1.5.2 Conjugate Gradient Method (CGM)

The CGM accelerates convergence by using conjugate directions [20, 17].

Algorithm 2 Conjugate Gradient Method for Inverse Problems

```
Initialize f^0, compute g^0 = J'(f^0), set d^0 = −g^0.
for k = 0, 1, 2, ... until stopping criterion do
    Perform line search to compute α_k.
    Update f^{k+1} = f^k + α_k d^k.
    Compute new gradient g^{k+1} = J'(f^{k+1}).
    Compute β_k = ||g^{k+1}||^2 / ||g^k||^2.
    Update direction d^{k+1} = −g^{k+1} + β_k d^k.
end for
```

CGM typically converges in fewer iterations than Landweber, though it is more sensitive to noise.

1.5.3 Comparison

Landweber is robust but slow; CGM is fast but sensitive. Hybrid methods and Sobolev gradient approaches have been proposed to combine their advantages [17].

1.6 Controllability of Singular/Degenerate Equations

1.6.1 Carleman Estimates

Carleman estimates play a dual role, providing both observability inequalities for controllability and stability results for inverse problems. They are of the form

$$\int_{Q_T} e^{2s\varphi}(|\partial_t u|^2 + |\Delta u|^2)\, dxdt \leq C \int_{Q_T} e^{2s\varphi}|\mathcal{L}_\mu u|^2\, dxdt,$$

where φ is a weight function. Carleman estimates underpin both uniqueness in inverse problems and controllability [13, 26].

1.6.2 Observability Inequalities

Observability inequalities link the norm of the solution at initial time to integrals over a control region:

$$\|\psi(\cdot, 0)\|^2_{L^2(\Omega)} \leq C \int_0^T \int_\omega |\psi(x,t)|^2 dxdt.$$

These inequalities are equivalent to null controllability of the forward equation.

1.6.3 Null Controllability

A singular/degenerate parabolic equation is null controllable if one can drive any initial state to zero at time T using controls supported in ω. Results in this direction combine Carleman estimates with Hardy inequalities [1, 2].

1.6.4 Applications

Controllability results apply to:

- Heat conduction with singular potentials.

- Population dynamics with spatial heterogeneity.
- Diffusion in heterogeneous or porous media.
- Inverse problems, where observability inequalities yield stability estimates.

1.7 Conclusion

This chapter has reviewed the state of the art in functional analysis, optimization, numerical identification, and controllability for singular/degenerate parabolic equations. Functional analytic tools (Sobolev spaces, Hardy inequalities) provide the framework; fractional calculus and singular operators extend classical diffusion models. Optimization and variational methods reformulate inverse problems into tractable forms, solved numerically by iterative regularization methods such as Landweber and CGM. Controllability theory, via Carleman estimates and observability inequalities, establishes null controllability and strengthens uniqueness and stability results in inverse problems.

Together, these tools form the theoretical and numerical foundation upon which this thesis builds to obtain new results on uniqueness, stability, and numerical reconstruction in singular parabolic models.

Chapter 2

Inverse Source Recovery in a Class of Singular Diffusion Equations via Optimal Control

2.1 introduction

Inverse problems are concerned with the identification of unknown inputs or sources from partial or indirect observations of the system's response, in contrast to forward problems, where the output is computed from given inputs. It is well known that inverse problems are often ill-posed in the sense of Hadamard; that is, the solution may not exist, may not be unique, or may not depend continuously on the data. Consequently, small perturbations in the measurements—such as those due to noise—can lead to significant errors in the solution

In the present work, we investigate the inverse problem of identifying a spatially dependent source term in a singular parabolic equation from measurements of the solution at a fixed final time. More precisely, we consider the following initial-boundary value problem

$$\begin{cases} \partial_t u(x,t) - u_{xx}(x,t) - \dfrac{\mu}{|x|^2} u(x,t) = f(x), \quad (x,t) \in Q_T := \Omega \times (0,T), \\ u(0,t) = u(1,t) = 0, \quad t \in (0,T), \\ u(x,0) = u_0(x), x \in \Omega, \end{cases} \tag{2.1}$$

where $\Omega := (0,1)$, $0 < T < \infty$ is an arbitrary final fixed time, u_0 is a given smooth function describe the initial state, $f(x)$ represents the unknown source term which is assumed to be kept independent of time variable t.

We are particularly concerned with the inverse problem of recovering the spatially dependent source term $f(x)$ appearing in the governing parabolic equation. To this end, we assume that the solution $u(x,t)$ is observed at the final time $t = T$ over the spatial domain Ω, that is,

$$u(x,T) = \omega(x), \quad x \in \Omega, \tag{2.2}$$

where $\omega \in L^2(\Omega)$ denotes the final-time observation. When the source term $f(x)$ is known, the associated initial-boundary value problem (2.1) defines the so-called direct (or forward) problem. In the present study, however, $f(x)$ is unknown and must be identified from the final observation (2.2). Accordingly, we formulate the inverse problem as the determination of $f(x)$ from a prescribed admissible class such that the corresponding solution to (2.1) satisfies the final-time constraint (2.2).

Singular inverse-square potentials have attracted considerable attention in recent years due to their relevance in modeling various physical phenomena across multiple disciplines, including quantum cosmology [12], combustion theory [9], electron capture processes [22], and quantum mechanics [16]. Moreover, such potentials naturally arise in the linearization of certain reaction–diffusion systems governed by the heat equation involving supercritical source terms [15].

In the context of inverse problems for parabolic equations, a substantial body of literature has addressed issues related to stability and well-posedness for various classes of equations using a range of analytical and numerical techniques [31, 58, 57, 27, 14, 54].

Concerning inverse problems for singular parabolic equations, we mention, among other works, the study in [48], where the inverse source problem for the model (2.1) was investigated in a multidimensional setting. In [5], the author addressed the inverse problem of identifying a source term in degenerate singular parabolic equations, with degeneracy and singularity occurring in the interior of the spatial domain. More recently, in [45], the inverse source problem for a heat equation involving multipolar inverse-square potentials was considered.

From a numerical perspective, it is worth noting that only a limited number of works have been devoted to the identification of source terms or coefficients in parabolic equations with inverse-square potentials, despite the fact that such models arise naturally in both theoretical studies and applied contexts.

In contrast to the aforementioned studies, which commonly rely on techniques based on Carleman estimates [27], our approach is framed within the context of optimal control theory a widely used methodology for addressing inverse source problems in a broad class of evolution equations [15, 4, 42, 56]. To overcome the ill-posedness of this inverse source problem, we adopt an optimal control framework, which provides both regularization and a systematic way to establish existence, uniqueness, and stability results. Specifically, we recast the inverse problem as an optimal control problem, where the unknown source term is treated as a control variable. The objective is then to minimize a suitably defined cost functional, which yields a quasi-solution to the original inverse problem.

By deriving and analyzing the first-order necessary optimality conditions, we establish both the local stability and uniqueness of the quasi-solution. More precisely, our main stability result can be stated as follows: let (U, f) and $(\tilde{U}, \tilde{f})$ be two solutions to the inverse problem (2.1)–(2.2) corresponding to final-time observations ω and $\tilde{\omega}$, respectively. Then, there exists a constant $C > 0$, independent of the final time T, such that

$$\|f - \tilde{f}\|^2_{L^2(\Omega)} \leq C\|\omega - \tilde{\omega}\|^2_{L^2(\Omega)}.$$

The second main contribution of this chapter concerns the numerical reconstruction of the unknown source term in the problem (2.1), based on the final-time observation (2.2). To this end, we develop a numerical scheme built upon the well-known Landweber iterative method. This approach has proven to be both reliable and efficient, as demonstrated through a series of numerical experiments.

The remainder of the chapter is organized as follows. In Section 2, we establish the well-posedness of the direct problem (2.1). Section 3 is devoted to the analysis of the inverse problem within an optimal control framework; in particular, we prove the existence of a minimizer for the cost functional and derive the associated first-order necessary optimality condition. In Section 4, using the optimality condition, we establish a stability result for the inverse problem. Section 5 is concerned with the numerical reconstruction of the unknown source term. To this end, we implement a Landweber-type iterative method to compute an approximate solution to the inverse problem based on the final-time data.

2.2 Analysis of the direct problem

2.2.1 Functional framework

As is well known in the analysis of parabolic equations involving singular inverse-square potentials, the constant μ plays a crucial role in determining the well-posedness of the associated problem. Specifically, there exists a critical threshold $\mu^* > 0$ beyond which the problem becomes ill-posed. This upper bound is given by the optimal constant in the Hardy inequality, which ensures that for any function $z \in H_0^1(\Omega)$, the weighted function $\frac{z}{x} \in L^2(\Omega)$, and the following inequality holds:

$$\mu^* \int_\Omega \frac{z^2(x)}{x^2}\, dx \leq \int_\Omega |z_x(x)|^2\, dx. \tag{2.3}$$

In the one-dimensional setting $\Omega = (0,1)$, it is known that the critical constant is $\mu^* = \frac{1}{4}$. For fixed $\mu \in (0, \mu^*]$, we define the following functional space:

$$H^1_{\mu,0}(\Omega) := \{z \in H_0^1(\Omega) : \int_\Omega \left(z_x^2(x) - \mu \frac{z^2(x)}{x^2} \right) dx < +\infty\}.$$

This space is a Hilbert space when equipped with the inner product

$$(z_1, z_2)_\mu := \int_\Omega \left(z_{1,x}(x) z_{2,x}(x) - \mu \frac{z_1(x) z_2(x)}{x^2} \right) dx,$$

and the corresponding norm

$$\|z\|_\mu := \left(\int_\Omega \left(z_x^2(x) - \mu \frac{z^2(x)}{x^2} \right) dx \right)^{1/2}.$$

By standard arguments, one can show that there exist positive constants $C_1, C_2 > 0$, depending on μ, such that

$$(1 - 4\mu) \int_\Omega z_x^2\, dx + C_1 \int_\Omega z^2\, dx \leq \|z\|_\mu^2 \leq (1 + 4\mu) \int_\Omega z_x^2\, dx + C_2 \int_\Omega z^2\, dx.$$

This implies that for the subcritical case $\mu < \mu^*$, the spaces $H^1_{\mu,0}(\Omega)$ and $H_0^1(\Omega)$ are topologically equivalent with respect to their norms. However, in the critical case $\mu = \mu^*$, the space $H^1_{\mu,0}(\Omega)$ strictly contains $H_0^1(\Omega)$, that is,

$$H_0^1(\Omega) \subsetneq H^1_{\mu,0}(\Omega).$$

In this work, we restrict our analysis to the subcritical case $0 < \mu < \mu^*$.for which coercivity and compactness properties hold, ensuring the well-posedness of the direct problem. Now, let us define the space $H^1_\mu(\Omega)$ as the completion of $H^1(\Omega)$ with respect to the norm

$$\|z\|_{H^1_\mu(\Omega)} := \left(\|z\|^2_{L^2(\Omega)} + \|z\|^2_\mu \right)^{1/2}.$$

Accordingly, we may write

$$H^1_{\mu,0}(\Omega) = \left\{ z \in H^1_\mu(\Omega) \,:\, z(0) = z(1) = 0 \right\}.$$

Under the assumption $\mu < \frac{1}{4}$, it is known that $H^1_\mu(\Omega)$ embeds continuously into the Sobolev space $W^{1,q}_0(\Omega)$ for all $1 \leq q < 2$, and also into the fractional Sobolev spaces $H^s_0(\Omega)$ for all $0 \leq s < 1$. Moreover, due to the compact embedding $W^{1,q}_0(\Omega) \hookrightarrow H^s_0(\Omega)$ for suitable $q = q(s)$ sufficiently close to 2, and the compactness of $H^s_0(\Omega) \hookrightarrow L^2(\Omega)$, we conclude that

$$H^1_\mu(\Omega) \hookrightarrow\hookrightarrow L^2(\Omega),$$

where the embedding is compact. For more details on the properties of $H^1_\mu(\Omega)$, we refer the reader to [3] and [?].

2.2.2 Well-posedness of the Direct Problem

In order to analyze the inverse problem associated with the differential equation under consideration, a thorough understanding of the corresponding direct problem is essential. Therefore, we begin by establishing the well-posedness of the direct problem, with a detailed analysis of the existence, uniqueness, and regularity of its solutions.

We now introduce the notion of weak solution adapted to the singular operator, we multiply equation (2.1) by a test function $\phi \in H^1_{\mu,0}(\Omega)$, integrate over Ω, and use integration by parts. This leads to the following variational formulation.

Definition 2.1. Let $u_0 \in L^2(\Omega)$ and $f \in L^2(Q_T)$. A function u is said to be a *weak solution* to problem (2.1) if

$$u \in L^2(0,T; H^1_{\mu,0}(\Omega)), \quad u_t \in L^2(0,T; H^{-1}_\mu(\Omega)),$$

and for all test functions $\phi \in L^2(0,T; H^1_{\mu,0}(\Omega))$, the following variational identity holds:

$$\iint_{Q_T} u_t \phi \, dx \, dt + \iint_{Q_T} u_x \phi_x \, dx \, dt - \mu \iint_{Q_T} \frac{u\phi}{x^2} \, dx \, dt = \iint_{Q_T} f \phi \, dx \, dt, \quad (2.4)$$

with the initial condition $u(0) = u_0$ satisfied in $L^2(\Omega)$.

Remark 2.2. The use of the weighted Sobolev space $H^1_{\mu,0}(\Omega)$ is crucial due to the singularity of the potential term $\mu x^{-2} u$, which renders the classical space $H^1_0(\Omega)$ inadequate when $\mu > 0$. For $\mu < \mu^*$, the Hardy inequality ensures that the bilinear form associated with the operator is coercive on $H^1_{\mu,0}(\Omega)$.

Theorem 2.3. *Let $u_0 \in L^2(\Omega)$ and $f \in L^2(Q_T)$. Then, problem* (2.1) *admits a unique weak solution θ in the sense of Definition 2.1, satisfying*

$$u \in C([0,T]; L^2(\Omega)) \cap L^2(0,T; H^1_{\mu,0}(\Omega)), \quad u_t \in L^2(0,T; H^{-1}_\mu(\Omega)).$$

Moreover, the following a priori energy estimate *holds:*

$$\sup_{t\in[0,T]} \|u(t)\|^2_{L^2(\Omega)} + \int_0^T \|u(t)\|^2_\mu \, dt + \int_0^T \|u_t(t)\|^2_{H^{-1}_\mu(\Omega)} \, dt \le C \left(\|u_0\|^2_{L^2(\Omega)} + \|f\|^2_{L^2(Q_T)} \right), \tag{2.5}$$

where the constant $C > 0$ depends only on μ, Ω, and T.

2.3 Optimal control

The inverse problem under consideration is ill-posed in the sense of Hadamard, meaning that uniqueness and stability of solutions cannot be guaranteed without introducing additional constraints.
A widely used strategy in such cases is to recast the inverse problem as an optimal control problem, where the unknown source term is treated as a control variable.
This approach allows us to incorporate a regularization mechanism that stabilizes the inversion procedure.

More precisely, the inverse problem is reformulated as the minimization of a Tikhonov-type cost functional, consisting of two terms: a data misfit term that enforces consistency with the final-time observation, and a penalty term that ensures stability by controlling the norm of the source.
The admissible set of controls is restricted to bounded functions in $L^2(\Omega)$, which reflects a priori physical knowledge about the source.

This optimal control formulation serves as the foundation for the subsequent analysis. In particular, it allows us to establish the existence of minimizers (**Th**2), to derive necessary optimality conditions (**Th**3), and to prove stability estimates for the reconstructed source (**Th**4). Hence, Section 3 plays a crucial role in bridging the direct analysis of the forward problem with the theoretical and numerical treatment of the inverse problem.

2.4 Formulation of the Inverse Problem

The inverse problem addressed in this work can be stated as follows: given an initial condition $u_0(x) \in L^2(\Omega)$ and a final-time observation $\omega(x) \in L^2(\Omega)$, determine the spatially dependent source term $f(x)$ such that the corresponding solution u to the initial-boundary value problem (2.1) satisfies the over-specified final condition

$$u(x,T) = \omega(x), \quad \text{for all } x \in \Omega. \tag{2.6}$$

To tackle this ill-posed problem, we adopt an optimal control framework. The inverse problem is reformulated as the following constrained optimization problem: find $f^* \in \mathcal{A}$ such that

$$\min_{f\in\mathcal{A}} \mathcal{J}(f) = \mathcal{J}(f^*), \quad \text{subject to } u[f] \text{ solving (2.1)}, \tag{2.7}$$

where the cost functional $\mathcal{J} : L^2(\Omega) \to \mathbb{R}$ is defined by

$$\mathcal{J}(f) := \frac{1}{2}\, \|u[f](\cdot,T) - \omega\|^2_{L^2(\Omega)} + \frac{\gamma}{2}\|f\|^2_{L^2(\Omega)}, \tag{2.8}$$

and $\gamma > 0$ is a regularization parameter. The admissible set $\mathcal{A} \subset L^2(\Omega)$ is given by

$$\mathcal{A} := \left\{ f \in L^2(\Omega) \,:\, c_0 \le f(x) \le c_1 \text{ a.e. in } \Omega \right\}, \tag{2.9}$$

for some constants $0 < c_0 < c_1$. The regularization term in (2.8) ensures the stability of the minimization problem and reflects a priori bounds on the unknown source.

Next, we establish the existence of an optimal solution to the minimization problem (2.7) by means of the following result.

Theorem 2.4. *Let $u_0 \in L^2(\Omega)$, $\omega \in L^2(\Omega)$, and assume that the direct problem* (2.1) *admits a unique weak solution $u[f]$ for every $f \in \mathcal{A}$, as guaranteed by **Theorem** 2.3. Then, the optimal control problem* (2.7) *admits at least one solution; that is, there exists $f^* \in \mathcal{A}$ such that*

$$\mathcal{J}(f^*) = \min_{f\in\mathcal{A}} \mathcal{J}(f).$$

Proof. The proof relies on the direct method of the calculus of variations, combining compactness, weak convergence, and lower semicontinuity arguments.

Since $\mathcal{J}(f) \ge 0$ for all $f \in \mathcal{A}$, the cost functional $\mathcal{J}$ admits an infimum over the admissible set $\mathcal{A}$, denoted by

$$d := \inf_{f\in\mathcal{A}} \mathcal{J}(f).$$

Let $(f_n)_{n\in\mathbb{N}} \subset \mathcal{A}$ be a minimizing sequence such that

$$d < \mathcal{J}(f_n) \le d + \frac{1}{n}, \quad \text{for all } n \in \mathbb{N}^*. \tag{2.10}$$

Since $\mathcal{A} \subset L^2(\Omega)$ is closed, convex, and bounded, there exists a subsequence (still denoted f_n) and a limit $f^* \in \mathcal{A}$ such that

$$f_n \rightharpoonup f^* \quad \text{weakly in } L^2(\Omega). \tag{2.11}$$

Let $u_n := u[f_n]$ denote the unique weak solution to problem (2.1) with source term f_n. By Theorem 2.3, the sequence (u_n) is uniformly bounded in the spaces

$$L^2(0,T;H^1_{\mu,0}(\Omega)), \quad L^\infty(0,T;L^2(\Omega)), \quad \text{and} \quad L^2(0,T;H^{-1}_\mu(\Omega)).$$

Hence, up to a subsequence, there exists $u^* \in L^2(0,T;H^1_{\mu,0}(\Omega))$ such that

$$\begin{aligned} &u_n \rightharpoonup u^* \quad \text{weakly in } L^2(0,T;H^1_{\mu,0}(\Omega)), \\ &u_n \overset{*}{\rightharpoonup} u^* \quad \text{weakly-* in } L^\infty(0,T;L^2(\Omega)), \\ &\partial_t u_n \rightharpoonup \partial_t u^* \quad \text{weakly in } L^2(0,T;H^{-1}_\mu(\Omega)). \end{aligned} \tag{2.12}$$

Furthermore, by the Aubin–Lions lemma and the compact embedding $H^1_{\mu,0}(\Omega) \hookrightarrow\hookrightarrow L^2(\Omega)$, we also obtain the strong convergence

$$u_n \to u^* \quad \text{strongly in } L^2(Q_T). \tag{2.13}$$

Now, subtracting the weak formulations satisfied by $u^* = u[f^*]$ and $u_n = u[f_n]$, and testing the resulting equation by $\phi = u^* - u_n$, we obtain the energy inequality:

$$\frac{1}{2}\frac{d}{dt}\|u^*(t) - u_n(t)\|^2_{L^2(\Omega)} \leq h(t) \int_\Omega (f^*(x) - f_n(x))(u^*(x,t) - u_n(x,t))\,dx. \tag{2.14}$$

Integrating both sides over $(0,T)$, we get

$$\|u^*(T) - u_n(T)\|^2_{L^2(\Omega)} \leq \iint_{Q_T} h(t)(f^*(x) - f_n(x))(u^*(x,t) - u_n(x,t)u)\,dx\,dt.$$

Using the weak convergence $f_n \rightharpoonup f^*$ in $L^2(\Omega)$ and strong convergence $u_n \to u^*$ in $L^2(Q_T)$, we deduce that the right-hand side vanishes as $n \to \infty$, hence:

$$\|u^*(T) - u_n(T)\|_{L^2(\Omega)} \to 0 \quad \text{as } n \to \infty. \tag{2.15}$$

To conclude, we analyze the convergence of the misfit term. Define:

$$\begin{aligned} I_n &:= \left| \|u^*(T) - \omega\|^2_{L^2(\Omega)} - \|u_n(T) - \omega\|^2_{L^2(\Omega)} \right| \\ &\leq \|u^*(T) - u_n(T)\|_{L^2(\Omega)} \cdot \|u^*(T) + u_n(T) - 2\omega\|_{L^2(\Omega)}. \end{aligned}$$

Due to (2.15), we conclude:

$$\lim_{n\to\infty} \|u_n(T)-\omega\|^2_{L^2(\Omega)} = \|u^*(T)-\omega\|^2_{L^2(\Omega)}. \tag{2.16}$$

Finally, applying weak lower semi-continuity of the L^2-norm to (2.11), and using (2.16), we obtain:

$$\begin{aligned}\liminf_{n\to\infty} \mathcal{J}(f_n) &= \liminf_{n\to\infty}\left(\frac{1}{2}\|u_n(T)-\omega\|^2 + \frac{\gamma}{2}\|f_n\|^2\right)\\ &\geq \frac{1}{2}\|u^*(T)-\omega\|^2 + \frac{\gamma}{2}\|f^*\|^2 = \mathcal{J}(f^*).\end{aligned}$$

Combining this with the minimality of the sequence (2.10), we conclude that f^* is indeed a minimizer of the functional $\mathcal{J}$, i.e., $\mathcal{J}(f^*) = d$. This completes the proof. □

Theorem 2.5. *Let $f^* \in \mathcal{A}$ be an optimal solution to the control problem* (2.7)*, and let $u^* := u[f^*]$ denote the corresponding solution to the state equation* (2.1)*. Then, the following variational inequality holds:*

$$\int_\Omega [u^*(x,T)-\omega(x)]\,\xi(x,T)\,dx + \gamma\int_\Omega f^*(x)\,(h(x)-f^*(x))\,dx \geq 0, \quad \forall h \in \mathcal{A}, \tag{2.17}$$

where $\xi \in L^2(0,T;H^1_{\mu,0}(\Omega)) \cap C([0,T];L^2(\Omega))$ is the unique weak solution to the following adjoint problem:

$$\begin{cases} \partial_t\xi(x,t) - \xi_{xx}(x,t) - \dfrac{\mu}{x^2}\xi(x,t) = h(x) - f^*(x), & \text{in } Q_T := \Omega\times(0,T),\\ \xi(0,t) = \xi(1,t) = 0, & \text{for } t \in (0,T),\\ \xi(x,0) = 0, & \text{for } x \in \Omega := (0,1). \end{cases} \tag{2.18}$$

Proof. Let $h \in \mathcal{A}$ and $\delta \in [0,1]$, and define a convex perturbation of the optimal control f^* by

$$f_\delta := f^* + \delta(h - f^*).$$

Since $\mathcal{A}$ is convex, it follows that $f_\delta \in \mathcal{A}$ for all $\delta \in [0,1]$. Let $u_\delta := u[f_\delta]$ denote the unique weak solution to problem (2.1) associated with the control f_δ.

We define the perturbed cost functional

$$\mathcal{J}_\delta := \mathcal{J}(f_\delta) = \frac{1}{2}\int_\Omega |u_\delta(x,T)-\omega(x)|^2 dx + \frac{\gamma}{2}\int_\Omega |f_\delta(x)|^2 dx. \tag{2.19}$$

Since f^* is an optimal control, the function $\delta \mapsto \mathcal{J}(f_\delta)$ attains its minimum at $\delta = 0$. Therefore, the derivative of $\mathcal{J}_\delta$ with respect to δ satisfies

$$\frac{d}{d\delta}\mathcal{J}(f_\delta)\bigg|_{\delta=0} \geq 0. \tag{2.20}$$

We now compute this derivative. By differentiating under the integral sign and using the chain rule, we obtain:

$$\frac{d}{d\delta}\mathcal{J}(f_\delta) = \int_\Omega [u_\delta(x,T) - \omega(x)]\,\frac{\partial u_\delta}{\partial \delta}(x,T)\,dx + \gamma\int_\Omega f_\delta(x)(h(x) - f^*(x))\,dx. \tag{2.21}$$

Evaluating (2.21) at $\delta = 0$, we define $\xi := \frac{\partial u_\delta}{\partial \delta}\big|_{\delta=0}$.
Then inequality (2.20) becomes:

$$\int_\Omega [u^*(x,T) - \omega(x)]\,\xi(x,T)\,dx + \gamma\int_\Omega f^*(x)(h(x) - f^*(x))\,dx \geq 0, \tag{2.22}$$

which is precisely the desired variational inequality (2.17).

It remains to characterize ξ. Differentiating the state equation with respect to δ, we find that ξ satisfies the following linearized problem:

$$\begin{cases} \partial_t\xi(x,t) - \xi_{xx}(x,t) - \dfrac{\mu}{x^2}\xi(x,t) = h(x) - f^*(x), & \text{in } Q_T,\\ \xi(0,t) = \xi(1,t) = 0, & t \in (0,T),\\ \xi(x,0) = 0, & x \in \Omega, \end{cases}$$

which coincides with problem (2.18). This concludes the proof. □

2.5 Stability Results

In this section, we investigate the stability of the inverse problem with respect to perturbations in the final-time observation data. Stability plays a central role in inverse problems, especially due to their inherent ill-posedness in the sense of Hadamard. In our context, the goal is to assess how the optimal solution f^* depends continuously on the measured data $\omega \in L^2(\Omega)$.

We consider two final-time observations $\omega, \tilde{\omega} \in L^2(\Omega)$, and analyze the corresponding solutions $f^*, \tilde{f}^* \in \mathcal{A}$ obtained by minimizing the cost functional (2.7). Under appropriate assumptions, we prove that small perturbations in the data lead to small changes in the recovered source, thereby establishing a Lipschitz-type stability estimate for the inverse problem.

Theorem 2.6. *Let $f, \tilde{f} \in \mathcal{A}$ be two optimal controls corresponding to the final observations $\omega, \tilde{\omega} \in L^2(\Omega)$, respectively, and let $u := u[f]$, $\tilde{u} := u[\tilde{f}]$ be the associated solutions to the state equation* (2.1)*. Then, the following Lipschitz-type stability estimate holds:*

$$\|f - \tilde{f}\|^2_{L^2(\Omega)} \leq \frac{1}{2\gamma}\|\omega - \tilde{\omega}\|^2_{L^2(\Omega)}. \tag{2.23}$$

Proof. Let $f, \tilde{f} \in \mathcal{A}$ be two optimal controls corresponding to the final-time data $\omega, \tilde{\omega} \in L^2(\Omega)$, and let $u := u[f]$, $\tilde{u} := u[\tilde{f}]$ be the associated solutions to the state problem (2.1).

We apply the first-order optimality condition (2.17) with $f^* = f$ and $h = \tilde{f}$, yielding:

$$\int_\Omega [u(x,T) - \omega(x)]\, \xi(x,T)\, dx + \gamma \int_\Omega f(x)(\tilde{f}(x) - f(x))\, dx \geq 0, \tag{2.24}$$

where ξ solves the adjoint problem:

$$\begin{cases} \partial_t \xi - \xi_{xx} - \dfrac{\mu}{x^2}\xi = \tilde{f} - f, & \text{in } Q_T, \\ \xi(0,t) = \xi(1,t) = 0, & t \in (0,T), \\ \xi(x,0) = 0, & x \in \Omega. \end{cases} \tag{2.25}$$

Similarly, applying (2.17) with $f^* = \tilde{f}$ and $h = f$, we obtain:

$$\int_\Omega [\tilde{u}(x,T) - \tilde{\omega}(x)]\, \tilde{\xi}(x,T)\, dx + \gamma \int_\Omega \tilde{f}(x)(f(x) - \tilde{f}(x))\, dx \geq 0, \tag{2.26}$$

where $\tilde{\xi}$ solves:

$$\begin{cases} \partial_t \tilde{\xi} - \tilde{\xi}_{xx} - \dfrac{\mu}{x^2}\tilde{\xi} = f - \tilde{f}, & \text{in } Q_T, \\ \tilde{\xi}(0,t) = \tilde{\xi}(1,t) = 0, & t \in (0,T), \\ \tilde{\xi}(x,0) = 0, & x \in \Omega. \end{cases} \tag{2.27}$$

Adding inequalities (2.24) and (2.26) yields:

$$\gamma\|f - \tilde{f}\|^2_{L^2(\Omega)} \leq \int_\Omega [u(T) - \omega]\, \xi(T)\, dx + \int_\Omega [\tilde{u}(T) - \tilde{\omega}]\, \tilde{\xi}(T)\, dx. \tag{2.28}$$

Now, define the error functions $E := u - \tilde{u}$, and $X := \xi - \tilde{\xi}$. Then, E solves:

$$\begin{cases} \partial_t E - E_{xx} - \dfrac{\mu}{x^2}E = f - \tilde{f}, & \text{in } Q_T, \\ E(0,t) = E(1,t) = 0, & t \in (0,T), \\ E(x,0) = 0, & x \in \Omega, \end{cases} \tag{2.29}$$

and X solves the homogeneous problem:

$$\begin{cases} \partial_t X - X_{xx} - \dfrac{\mu}{x^2} X = 0, & \text{in } Q_T, \\ X(0,t) = X(1,t) = 0, & t \in (0,T), \\ X(x,0) = 0, & x \in \Omega. \end{cases} \tag{2.30}$$

Hence, by uniqueness of weak solutions, we conclude $X = 0$, i.e., $\xi = \tilde{\xi}$, and similarly $E = -\xi$ from comparing (2.29) and (2.25).

Substituting into (2.28) and using $E = -\xi$, we obtain:

$$\begin{aligned} \gamma \|f - \tilde{f}\|^2 &\leq \int_\Omega E(x,T)\xi(x,T)\,dx + \int_\Omega (\omega(x) - \tilde{\omega}(x))\xi(x,T)\,dx \\ &= -\|\xi(\cdot,T)\|^2_{L^2(\Omega)} + \int_\Omega (\omega - \tilde{\omega})\xi(\cdot,T)\,dx. \end{aligned}$$

Applying the Cauchy–Schwarz and Young inequalities, we get:

$$\begin{aligned} \gamma \|f - \tilde{f}\|^2 &\leq -\|\xi(T)\|^2 + \|\omega - \tilde{\omega}\| \cdot \|\xi(T)\| \\ &\leq -\|\xi(T)\|^2 + \frac{1}{2}\|\omega - \tilde{\omega}\|^2 + \frac{1}{2}\|\xi(T)\|^2 \\ &= -\frac{1}{2}\|\xi(T)\|^2 + \frac{1}{2}\|\omega - \tilde{\omega}\|^2 \\ &\leq \frac{1}{2}\|\omega - \tilde{\omega}\|^2. \end{aligned}$$

Dividing both sides by $\gamma > 0$, we conclude:

$$\|f - \tilde{f}\|^2_{L^2(\Omega)} \leq \frac{1}{2\gamma}\|\omega - \tilde{\omega}\|^2_{L^2(\Omega)},$$

which completes the proof. $\square$

Corollary 2.7. *Assume that assumptions of Theorem* (2.6) *hold. Furthermore, suppose that ω matches $\tilde{\omega}$ over Ω then $f = \tilde{f}$*

2.6 Numerical identification

In this section, we present a numerical strategy for identifying the unknown source term $f(x)$ in the singular parabolic problem (2.1), based on the final-time observation $\omega(x)$.The numerical experiments presented in this section illustrate the theoretical stability results and validate the proposed optimal control approach. Due to the ill-posedness of the inverse problem, direct inversion is highly unstable, and regularization techniques are essential to obtain stable and meaningful numerical approximations.

To this end, we implement an iterative regularization scheme based on the classical Landweber method, which is widely used in inverse problems due to its simplicity and robustness. The approach consists of iteratively updating the source term by moving along the negative gradient direction of the cost functional (2.7), evaluated via the solution of the associated forward and adjoint problems.

2.6.1 Landweber iteration method

Let us define the input-output operator $\mathcal{T}$ associated with the parabolic problem (2.1), which maps a source term to the final-time state of the corresponding solution. For simplicity of computation, we assume the initial condition is homogeneous, i.e., $u_0 = 0$. Then, the operator $\mathcal{T}$ is given by:

$$\begin{aligned} \mathcal{T} \colon \; L^2(\Omega) &\longrightarrow H^1_{\mu,0}(\Omega), \\ f &\mapsto \mathcal{T} f := u[f](\cdot, T), \end{aligned}$$

where $u[f]$ denotes the weak solution to problem (2.1) with source term $f \in L^2(\Omega)$, and $u_0 = 0$ as initial data. In this framework, $\mathcal{T} f$ represents the output measurement at the final time $t = T$.

In view of the above considerations, our inverse problem can be equivalently reformulated as the operator equation

$$\text{Find } f^\dagger \in \mathcal{A} \text{ such that } \mathcal{T} f^\dagger = \omega,$$

where $\mathcal{T} \colon L^2(\Omega) \to H^1_{\mu,0}(\Omega)$ is the input-output operator defined in the previous subsection, and $\omega \in L^2(\Omega)$ denotes the measured final-time data. Formally, the exact solution $f^\dagger$ satisfies the associated normal equation

$$\mathcal{T}^* \mathcal{T} f^\dagger = \mathcal{T}^* \omega,$$

where $\mathcal{T}^*$ denotes the adjoint of the operator $\mathcal{T}$. This normal equation can be interpreted as a fixed-point problem of the form

$$f^\dagger = f^\dagger - \beta \, \mathcal{T}^* \left(\mathcal{T} f^\dagger - \omega \right),$$

where $\beta > 0$ is a relaxation parameter. Based on this formulation, we construct an iterative Landweber-type method to approximate $f^\dagger$. Starting from an initial guess $f_0 \in L^2(\Omega)$, the iteration proceeds as:

$$\begin{aligned} f_{m+1} &= f_m - \beta \, \mathcal{T}^* \left(\mathcal{T}(f_m) - \omega \right) \\ &= f_m - \beta \, \mathcal{T}^* \left(u_m(\cdot, T) - \omega \right), \end{aligned} \tag{2.31}$$

where $u_m := u[f_m]$ is the solution of the forward problem (2.1) associated with the current iterate f_m.

It is well known (see, e.g., [18]) that the Landweber iteration (2.31) converges strongly to the minimum-norm solution $f^\dagger$, provided that $0 < \beta < 1/\|\mathcal{T}\|^2$ and the initial guess $f_0 \in \mathcal{D}(\mathcal{T})$. In practice, the iteration is terminated according to a suitable discrepancy principle or tolerance-based stopping rule.

Lemma 2.8. *Let $\psi \in L^2(\Omega)$, and let $\eta \in L^2(0,T;H^1_{\mu,0}(\Omega))$ be the unique weak solution of the following initial-boundary value problem:*

$$\begin{cases} \partial_t \eta(x,t) - \partial_{xx}\eta(x,t) + \dfrac{\mu}{x^2}\eta(x,t) = \psi(x), & \textit{in } Q_T := \Omega \times (0,T), \\ \eta(x,0) = 0, & x \in \Omega, \\ \eta(0,t) = \eta(1,t) = 0, & t \in (0,T). \end{cases} \tag{2.32}$$

Then, the adjoint operator $\mathcal{T}^*\colon L^2(\Omega) \to L^2(\Omega)$, corresponding to the input-output operator $\mathcal{T}f = u[f](\cdot,T)$, is given by

$$\mathcal{T}^*\psi = \eta(\cdot,T),$$

Proof. Let $f \in L^2(\Omega)$, and denote by $u = u[f] \in L^2(0,T;H^1_{\mu,0}(\Omega))$ the unique weak solution of the forward problem:

$$\begin{cases} \partial_t u(x,t) - \partial_{xx}u(x,t) + \dfrac{\mu}{x^2}u(x,t) = f(x), & \text{in } Q_T, \\ u(x,0) = 0, & x \in \Omega, \\ u(0,t) = u(1,t) = 0, & t \in (0,T). \end{cases} \tag{2.33}$$

Then the input-output operator $\mathcal{T}\colon L^2(\Omega) \to L^2(\Omega)$ is defined by

$$\mathcal{T}f = u(\cdot,T).$$

Let $\psi \in L^2(\Omega)$, and let $\eta \in L^2(0,T;H^1_{\mu,0}(\Omega))$ be the solution of the following adjoint problem:

$$\begin{cases} \partial_t \eta(x,t) - \partial_{xx}\eta(x,t) + \dfrac{\mu}{x^2}\eta(x,t) = \psi(x), & \text{in } Q_T, \\ \eta(x,0) = 0, & x \in \Omega, \\ \eta(0,t) = \eta(1,t) = 0, & t \in (0,T). \end{cases} \tag{2.34}$$

We want to compute $\mathcal{T}^*\psi$ using the definition of the adjoint. By definition, $\mathcal{T}^*$ is the operator such that

$$\langle \mathcal{T}f, \psi\rangle_{L^2(\Omega)} = \langle f, \mathcal{T}^*\psi\rangle_{L^2(\Omega)}, \quad \forall f \in L^2(\Omega).$$

Now, compute the left-hand side:

$$\langle \mathcal{T} f, \psi \rangle_{L^2(\Omega)} = \int_\Omega u(x,T)\psi(x)\, dx.$$

We aim to express this quantity in terms of f and η, and thereby identify $\mathcal{T}^*\psi$. To this end, we define the auxiliary function $v(x,t) := \eta(x, T-t)$. It is easy to verify (by direct substitution) that v satisfies the backward parabolic problem:

$$\begin{cases} -\partial_t v(x,t) - \partial_{xx} v(x,t) + \dfrac{\mu}{x^2} v(x,t) = \psi(x), & \text{in } Q_T, \\ v(x,T) = 0, & x \in \Omega, \\ v(0,t) = v(1,t) = 0, & t \in (0,T). \end{cases} \tag{2.35}$$

We now multiply the equation for u by v, integrate over Q_T, and use integration by parts in time and space. We obtain:

$$\begin{aligned} \iint_{Q_T} f(x) v(x,t)\, dxdt &= \iint_{Q_T} \left(\partial_t u \cdot v + \partial_x u \cdot \partial_x v + \frac{\mu}{x^2} uv \right) dxdt \\ &= \iint_{Q_T} \left(-\partial_t v \cdot u + \partial_x u \cdot \partial_x v + \frac{\mu}{x^2} uv \right) dxdt, \end{aligned}$$

where we have used the fact that $u(x,0) = v(x,T) = 0$.

Since v satisfies (2.35), the right-hand side becomes:

$$\iint_{Q_T} \psi(x) u(x,t)\, dxdt.$$

Thus, we have established the identity:

$$\iint_{Q_T} f(x) v(x,t)\, dxdt = \iint_{Q_T} \psi(x) u(x,t)\, dxdt.$$

Now, reversing the change of variables $v(x,t) = \eta(x, T-t)$, we have:

$$\int_0^T v(x,t)\, dt = \int_0^T \eta(x,s)\, ds.$$

Similarly,

$$\iint_{Q_T} f(x) v(x,t)\, dxdt = \int_\Omega f(x) \int_0^T \eta(x,s)\, ds\, dx,$$

and
$$\iint_{Q_T} \psi(x)u(x,t)\,dxdt = \int_\Omega \psi(x) \int_0^T u(x,t)\,dt\,dx.$$
Assuming that this identity holds for all $T > 0$, we formally differentiate both sides with respect to T, obtaining:

$$\int_\Omega \psi(x)u(x,T)\,dx = \int_\Omega f(x)\eta(x,T)\,dx.$$

Therefore, we have:

$$(\mathcal{T} f, \psi)_{L^2(\Omega)} = (u(\cdot,T), \psi)_{L^2(\Omega)} = (f, \eta(\cdot,T))_{L^2(\Omega)},$$

and since this holds for all $f \in L^2(\Omega)$, we conclude:

$$\mathcal{T}^* \psi = \eta(\cdot, T).$$

□

To summarize, we now outline the main steps of the iterative procedure used to numerically reconstruct the unknown source term f in problem (2.1), based on the Landweber method.

Algorithm 3 Iterative Landweber Method for Source Identification

Require: Relaxation parameter $\beta > 0$, tolerance $\varepsilon > 0$, final-time data $\omega \in L^2(\Omega)$

Ensure: Approximate solution $f^\dagger$ and corresponding state $u^\dagger$ to the inverse problem

Initialization: Choose initial guess $f_0 \in \mathcal{A}$, set $k = 0$

Solve Forward Problem: Compute $u_0 := u[f_0]$ by solving the forward equation

Solve Adjoint Problem: Compute η_0 by solving the adjoint equation with source $\psi = u_0(\cdot, T) - \omega$

Update Control: Set

$$f_1 := f_0 - \beta\eta_0(\cdot, T)$$

for $k = 1, 2, \ldots$ until convergence **do**
    Solve $u_k := u[f_k]$
    if $\|u_k(\cdot, T) - \omega\|_{L^2(\Omega)} < \varepsilon$ **then**
        Set $f^\dagger := f_k$, $u^\dagger := u_k$; **stop**
    else
        Solve η_k with $\psi = u_k(\cdot, T) - \omega$
        Update $f_{k+1} := f_k - \beta\eta_k(\cdot, T)$
    end if
end for

2.6.2 Numerical results and discussions

In this subsection, we present numerical experiments that illustrate the performance of the proposed Landweber algorithm for reconstructing the space-dependent source term. The experiments are designed to validate both the accuracy and stability of the method under noise-free and noisy final-time data.

We begin with Example 1, where the exact solution of the forward problem is available in closed form. This allows for a direct comparison between the reconstructed and exact source profiles. In Example 2, the forward solution is generated numerically, thereby testing the algorithm in a more realistic setting. In both cases, the reconstructions confirm the theoretical predictions: the Landweber method converges towards the true source when noise-free data are used, while in the presence of noisy data, the algorithm still yields stable and accurate approximations, as shown in Figures 6.1–6.3.

The relative error $E_2(k)$ is also monitored as a function of the iteration index k. The error curves demonstrate a rapid initial decrease followed by saturation, which is consistent with the discrepancy principle and the finite accuracy of the numerical discretization. Overall, these results validate the effectiveness and robustness of the proposed method. In the next chapter, we extend the inverse source reconstruction problem to time-fractional diffusion equations, where additional memory effects introduce new analytical challenges.

2.6.3 Numerical Implementation and Discretization

This subsection is devoted to numerical examples that illustrate the performance of the proposed Landweber algorithm for reconstructing the space-dependent source term $f(x)$ in the inverse problem (2.1). The solutions to both the direct and adjoint problems are approximated using finite-difference methods.

We fix the final time $T = 1$, so that the spatio-temporal domain is $Q_T = (0, 1) \times (0, 1)$. Let $M, N \in \mathbb{N}^*$ denote the number of spatial and temporal subdivisions, respectively. Define the mesh sizes

$$\Delta x = \frac{1}{M}, \quad \Delta t = \frac{1}{N}.$$

The spatial and temporal grid points are given by:

$$x_i = i\Delta x, \quad \text{for } i = 0, 1, \ldots, M, \qquad t_j = j\Delta t, \quad \text{for } j = 0, 1, \ldots, N.$$

The functions $u(x, t)$ (solution of the forward problem) and $\eta(x, t)$ (solution of the adjoint problem) are evaluated at these grid points. The numerical schemes employed for the discretization are based on finite-difference approximations of second-order spatial derivatives and backward or Crank–Nicolson schemes in time, ensuring stability in the presence of the singular potential μ/x^2. Boundary conditions are imposed explicitly at $x = 0$ and $x = 1$.

In the numerical tests, we measure the accuracy of the reconstructed source using the relative error at iteration k, defined by

$$E_2(k) := \|f^k - f\|^2_{L^2(\Omega)} = \frac{1}{M+1} \sum_{i=0}^{M} \left(f(x_i) - f^k(x_i)\right)^2,$$

where f is the exact source function and f^k is the reconstructed approximation at the k-th iteration, evaluated on the discrete grid $\{x_i\}_{i=0}^{M}$.

To test robustness against measurement errors, we also consider noisy data. The perturbed observation $\omega_\varepsilon(x)$ is generated from the exact final state $\omega(x) = \theta(x, T)$ by injecting a multiplicative random noise:

$$\omega_\varepsilon(x) = \omega(x) + \varepsilon \cdot \omega(x) \cdot \text{rand}(x), \quad x \in \Omega, \tag{2.36}$$

where $\varepsilon \in (0,1)$ denotes the noise level and $\mathrm{rand}(x) \in (0,1)$ is a uniformly distributed random function over the spatial domain. This simulates realistic data perturbations encountered in practice.

Example 2.9. In this first test case, we consider the inverse problem (2.1)–(2.2) with singularity parameter $\mu = \frac{1}{5}$, and a source term given by

$$f(x,t) = -5\sin(\pi t)\left((x^2 - \pi^2 x^2 + \mu)\sin(\pi x)\right), \quad (x,t) \in Q_T.$$

It is easy to verify that the corresponding exact solution of the forward problem (2.1) is

$$\theta(x,t) = x^2 \sin(\pi x)(1 - e^{-t}), \quad x \in \Omega, \quad t \in [0,T].$$

Consequently, the final-time observation used in the inverse problem is computed as $\omega(x) = u(x,T)$. This example allows for direct comparison between the reconstructed and exact source terms.

Example 2.10. In this second test, we consider a synthetic example in which the exact source term is prescribed as

$$f(x) = \sin(\pi x), \quad x \in \Omega.$$

We set the singularity parameter to $\mu = \frac{1}{6}$. The final-time data $\omega(x) = u(x,T)$ is generated by solving the direct problem (2.1) using this exact source. This test serves to validate the reconstruction algorithm when the forward solution is numerically simulated, without using an explicit expression for $u(x,t)$.

Discussion on Example 1

For the inversion process, we employ moderate discretization parameters, setting $\Delta t = 10^{-3}$ and $\Delta x = 5 \times 10^{-2}$. The Landweber iteration is initialized with the admissible guess $f_0(x) = x^2$. Figure 2.1 (a) shows a comparison between the exact source $f^\dagger$ and the reconstructed profile f_k in Example 1 after $k = 8000$ iterations. The agreement is notably close, confirming the convergence of the algorithm in the noise-free setting.

To assess the robustness of the method under measurement perturbations, we conduct additional experiments using noisy final-time data ω, generated according to the perturbation model (2.36). The reconstruction is evaluated after $k = 400$ iterations. As shown in Figure 2.2-(a), the reconstructions remain satisfactory under moderate noise levels, and the computed state

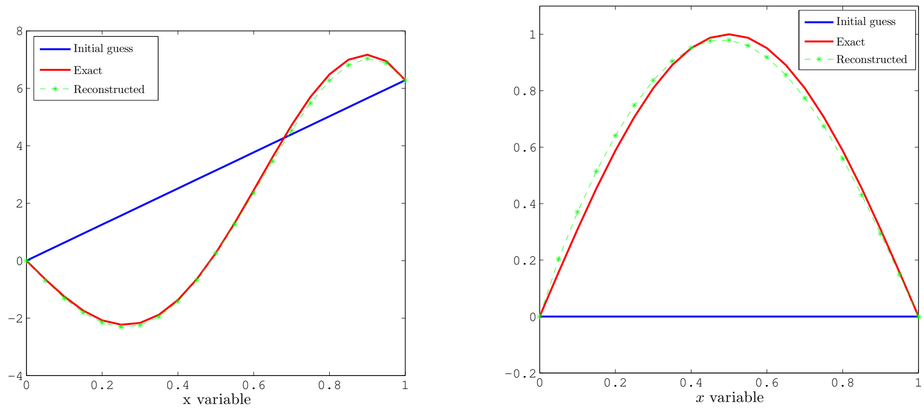

(a) Example 1 with $k = 800$ (b) Example 2 with $k = 400$

Figure 2.1: Numerical reconstruction.

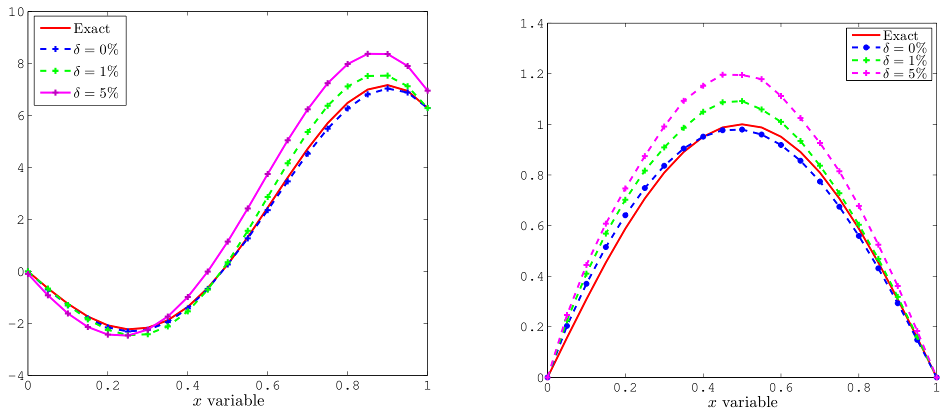

(a) Example 1 (b) Example 2

Figure 2.2: The numerical results with noise

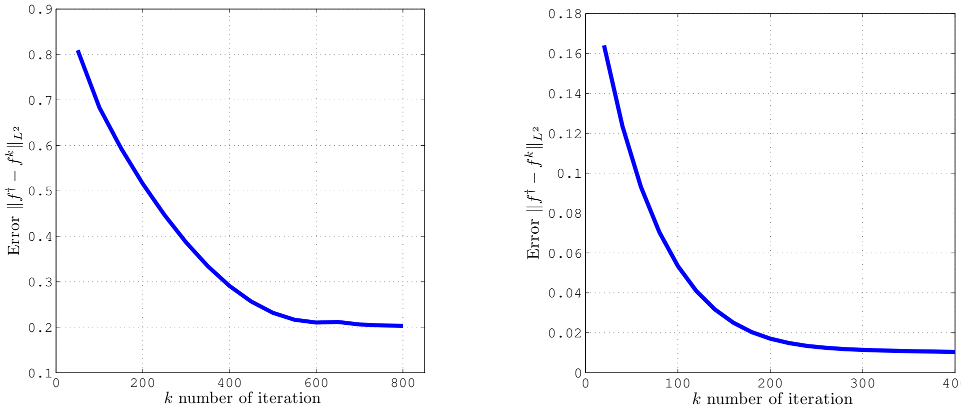

(a) Example 1 (b) Example 2

Figure 2.3: Behaviour of reconstruction error $E_2(k)$ as a function of k.

$\theta_k(\cdot, T)$ matches the perturbed observations ω with high accuracy. However, for higher noise levels, the reconstruction quality deteriorates significantly.

The evolution of $E_2(k)$ is shown in Figure 2.3-(a). We observe a monotonic decay of the error up to around $k = 400$, after which the reduction halts due to accumulated discretization errors in the numerical solution of the direct and adjoint problems.

Discussion on Example 2

For the second example, we consider a synthetic source term $f^\dagger(x) = \sin(\pi x)$ with singularity parameter $\mu = \frac{1}{6}$. The final-time observation $\omega(x)$ is generated by numerically solving the direct problem (2.1). The Landweber iteration is initialized with the same admissible guess $f_0(x) = 0$, and discretization parameters are set to $\Delta t = 10^{-3}$ and $\Delta x = 5 \times 10^{-2}$, as in the previous example. Figure 2.1 (b) displays the comparison between the exact source $f^\dagger$ and the reconstructed solution f_k after $k = 400$ iterations. The reconstruction achieves high accuracy with significantly fewer iterations than in Example 1, which is attributed to the simpler spectral content of the source.

To evaluate stability with respect to data perturbations, we introduce noisy observations based on the same noise model (2.36). The reconstruction after $k = 400$ iterations is reported in Figure 2.2 (b). The results indicate that the reconstructed state $\theta_k(\cdot, T)$ approximates the noisy data ω well for low to moderate noise levels. However, as the noise amplitude increases, the reconstruction degrades, consistent with the sensitivity of the inverse problem to measurement errors.

The convergence history of the relative error $E_2(k)$ is depicted in Figure 2.3 (b). Similar to the first example, we observe a rapid decay of the error up to $k \approx 300$, followed by stagnation. The early saturation is again due to the discretization effects and the finite resolution of the spatial grid, which limit further improvements in accuracy despite continued iteration.

Conclusion

In this work, we have addressed an inverse problem concerned with the identification of a space-dependent source term in a diffusion equation governed by a singular inverse-square potential. The proposed approach is based on an optimal control framework.

We began by establishing the existence and uniqueness of weak solutions to the direct problem. The inverse problem was then reformulated as a constrained optimization problem, for which we proved the existence of a minimizer and derived a first-order necessary optimality condition. This condition was further employed to demonstrate a Lipschitz-type stability result with respect to perturbations in the final-time data.

On the numerical side, we developed an iterative Landweber-type algorithm to reconstruct the unknown source term from noisy final measurements. A series of numerical experiments were carried out, confirming the effectiveness, stability, and robustness of the proposed reconstruction method, even in the presence of data perturbations.

As directions for future work, we plan to extend the current methodology to more complex models, including systems of coupled singular parabolic equations and fractional-order singular diffusion problems.

Chapter 3

Uniqueness and reconstruction of spatial sources in a time-fractional diffusion model with singular inverse-square potential

3.1 Introduction

Fractional diffusion models, also known as anomalous diffusion, have emerged as a topic of major interest due to their efficiency in modelling diffusion processes in complex media such as viscoelastic materials [38, 39], porous rocks [21], or biological tissues [36] , which often reveal behaviours that classical models fail to capture (see e.g. [24]). In contrast to ordinary (Brownian) diffusion, where the mean square displacement of particles grows linearly with time, $\langle x^2(t)\rangle \sim t$, experimental observations in various complex systems, such as plasmas and disordered media, have revealed deviations from this linear law. In these cases, the mean square displacement follows a fractional power-law behaviour in time, indicating the presence of memory and non-local effects. Such sub-diffusive motion is characterized by the asymptotic long-time relation $\langle x^2(t)\rangle \sim \frac{2K_\alpha}{\Gamma(1+\alpha)}t^\alpha$ as $t \to \infty$, where $0 < \alpha < 1$ denotes the anomalous diffusion exponent and K_α is the generalized diffusion coefficient.

With the growing advancement of studies devoted to exploring fractional-order models for describing anomalous diffusion, research has naturally shifted toward the investigation of inverse problems associated with these models, aiming at the reconstruction of unknown parameters or functions, from available observations obtained through additional measurements.

In this work, we investigate the direct and an inverse problems associated with a time-fractional diffusion equation involving a singular inverse-square potential. Let $\Omega := \Lambda \times (0,T)$ where $\Lambda := (0,1)$ and $T < \infty$ stands for a fixed final time. In this paper we are concerned with the following time-fractional diffusion model

$$\begin{cases} \partial_t^\alpha \theta(x,t) - \Delta\theta(x,t) - \frac{\mu}{x^2}\theta(x,t) = F(x,t), \quad (x,t) \in \Omega \\ \theta(x,0) = \theta_0(x), \quad x \in \Lambda \\ \theta(0,t) = \theta(1,t) = 0, \quad t \in (0,T) \end{cases} \tag{1.1}$$

where θ_0 is a regular function that describes the initial state, $\mu \in \mathbb{R}$ is a real parameter representing the strength of the inverse-square Hardy-type potential $V(x) = \frac{\mu}{x^2}$, and ${}_0\partial_t^\alpha$ denotes the left-hand sided Caputo fractional derivative defined for a smooth w by

$${}_0\partial_t^\alpha w(t) := \left(I_{0+}^{1-\alpha} \circ \partial_t\right) w(t) = \frac{1}{\Gamma(1-\alpha)} \int_0^t (t-s)^{-\alpha} \partial_s w(s) ds \tag{1.2}$$

where $\Gamma(\cdot)$ is the usual Gamma function and $I_{0+}^{1-\alpha}$ stands for the Riemann-Liouville fractional integral operator of order ($1-\alpha$), which is given explicitly as

$$I_{0+}^{1-\alpha} w(t) := \frac{1}{\Gamma(1-\alpha)} \int_0^t (t-s)^{-\alpha} w(s) ds \tag{1.3}$$

The source term $F(x,t)$ is assumed to be of separable form, that is, $F(x,t) = p(x)q(t)$ where $p(x)$ and $q(t)$ contribute the spatial and temporal components, respectively. If both p and q are known functions, then the problem is referred to as the forward problem, in which one seeks the solution $\theta(x,t)$ satisfying the governing equation and the associated initial and boundary conditions. However, when either p or q or both are unknown, the task of determining these functions from additional observations leads to an inverse source problem.

In this chapter we consider the following inverse problem for the time-fractional diffusion equation with separable source term.In contrast to the classical diffusion model studied in Chapter 2, the time-fractional diffusion equation incorporates memory effects that significantly influence both the analysis and the numerical reconstruction of inverse problems. Let $\Lambda \subset \mathbb{R}^n$ be a bounded domain and let $\theta = \theta(x,t;p)$ denote the solution of the forward problem corresponding to the spatial factor $p(x)$ (for fixed prescribed initial datum $\theta(\cdot,0)=\theta_0$ and time-dependent factor $q(t)$). Our observation is the final state

$$\theta(x,T)=\omega_{\text{obs}}(x), \quad x\in\Lambda \tag{1.4}$$

The inverse problem we study is:

$$(\mathbf{IP}):\begin{cases}\text{Given } \theta_0\in L^2(\Lambda), q\in L^\infty(0,T), \text{ and the final data } \omega_{\text{obs}}\in L^2(\Lambda),\\ \text{determine the spatial component } p\in L^2(\Lambda), \text{ such that } \theta[p](\cdot,T)=\omega_{\text{obs}}.\end{cases}$$

where $\theta(\cdot,t;p)$ denotes the solution of the forward problem corresponding to the parameter p.

Problems involving singular Hardy potentials play a fundamental role in several areas of analysis and mathematical physics. In combustion theory [**?**], it arises when modelling flame propagation in radially symmetric domains, where the inverse-square singularity captures the steep temperature gradient near the ignition source. In quantum mechanics [8], the Hardy potential appears in the study of Schrödinger operators with inverse-square perturbations, reflecting phenomena such as the fall-to-the-center instability and the breakdown of conformal invariance.

As is well known, when dealing with equations involving inverse-square potentials, the parameter μ plays a fundamental role. Although μ may, in principle, take any real value, it has been established (see, e.g. [**?**]) and the references therein) that there exists a critical value μ^* beyond which the corresponding problems become ill-posed. This critical value is determined by the optimal constant in the Hardy inequality, which guarantees that for every $z\in H_0^1(\Lambda)$, the product $x^{-1}z$ belongs to $L^2(\Lambda)$ and the following inequality holds

$$\mu^*\int_0^1\frac{z^2(x)}{x^2}dx\le\int_0^1|\nabla z(x)|^2dx \tag{1.5}$$

Indeed, in the one-dimensional case, the optimal constant in the Hardy inequality takes a sharp value $\mu^*=1/4$. In this paper, we restrict ourselves to the subcritical regime $\mu<\mu^*$, where such issues do not arise.

Recently, an increasing number of studies have been devoted to the theory of inverse problems for time-fractional diffusion equations. A substantial body of literature addresses these problems from multiple perspectives, including theoretical issues such as uniqueness, stability, and regularization, as well as numerical aspects, such as the development of efficient reconstruction algorithms (see [29] and references therein for an overview). This, reflects the importance of this research area in the broader context of applied mathematics and computational modelling. Indeed, inverse problems serve as powerful mathematical tools with wide-ranging applications in materials engineering, medical imaging, geophysics, and non-destructive testing, among other scientific and industrial fields.

Without being selective, we mention here, by way of example and not exhaustively, some of the approaches employed in this context, including Tikhonov regularization [19, 50], quasi-reversibility regularization method [10, 53] Landweber iterative method [52, 55], optimal control approaches [41, 46], quasi-boundaryvalue methods [51], and so on.

Nevertheless, a careful examination of the existing literature reveals that most of these studies have been confined to fractional models with regular coefficients and non-singular domains, whereas fractional equations involving singular potentials remain far less explored. To the best of our knowledge, the present work constitutes the first attempt to investigate an inverse problem for a time-fractional parabolic equation involving an inverse-square potential, addressing both the analytical properties of the forward problem and the numerical reconstruction of the unknown source term associated with such a singular setting.

This work presents a comprehensive investigation into the analysis and inversion of a time-fractional diffusion equation involving a singular inversesquare potential. The principal contributions of this study are threefold. First, we establish the well-posedness of a time-fractional diffusion equation with a singular inverse-square potential within an adequate variational framework. Furthermore, we derive essential regularity results for the solution, which are crucial for the subsequent analysis of the inverse problem. Second, we address the inverse problem of reconstructing an unknown spatial source term $p(x)$ from final-time data. Our main results concerns the unique identifiability of $p(x)$ under suitable conditions on the temporal component of the source, ensuring that the spatial term is uniquely determined by the terminal observation $\theta(x, T)$. Third, we develop a stable and efficient numerical reconstruction scheme based on Tikhonov regularization and the Conjugate Gradient Method. The Fréchet derivative of the Tikhonov functional is derived via an adjoint formulation, and the method's accuracy and robustness are validated through numerical experiments on both smooth and non-smooth sources under varying noise levels.

The paper is organized as follows. Section 2 is devoted to the analysis of the well-posedness of the forward problem within an appropriate variational framework. In addition, several auxiliary results concerning the regularity of weak solutions are established. In Section 3, we prove a uniqueness theorem for the identification of the spatial source term from final-time observations under suitable assumptions. Section 4 presents the construction of a stable numerical reconstruction scheme, where the inverse problem is reformulated as a Tikhonov-regularized optimization problem and efficiently solved by means of a Conjugate Gradient Method. The derivation of the corresponding adjoint problem is also provided in detail. In Section 5, a series of numerical experiments is carried out to demonstrate the accuracy, stability, and robustness of the proposed approach. Finally, concluding remarks and potential directions for future research are given in Section 6.

3.2 Analysis of the forward problem

3.2.1 Preliminaries

In this section, we shall recall and present some essential properties of fractional integrals and derivatives, as well as, introduce some fundamental definitions and results related to functional spaces that will be used throughout the paper.

Let ${}_0C^\infty(I)$ denotes the space of infinitely differentiable functions with compact support in $I := (0, T]$. Denote $L^2(\mathcal{D})$ as the space of square-integrable
functions over a domain $\mathcal{D}$, and its inner product and norm are given as follows

$$(\theta, \vartheta)_{0,\mathcal{D}} = \int_{\mathcal{D}} \theta(x)\vartheta(x)dx, \quad \|\theta\|^2_{0,\mathcal{D}} = \int_{\mathcal{D}} |\theta(x)|^2 dx$$

In addition to Caputo derivatives, we also employ the left- and right-sided Riemann-Liouville fractional derivatives, denoted respectively by ${}_0D_t^\alpha$ and D_T^α. (for further details, the reader is referred to [32]). Throughout this chapter, the time-fractional derivative is understood in the Caputo sense and is denoted by ${}_0D_t^\alpha$ with $\alpha \in (0, 1)$

Next, we shall introduce several definitions of fractional derivative spaces, which provide a suitable framework for establishing the well-posedness of the forward problem (see [34, 59]).

Definition 3.1. For $\alpha > 0$, we define the space

$$H_L^\alpha(I) := \left\{\theta \in L^2(I); {}_0D_t^\alpha\theta \in L^2(I)\right\}$$

Furthermore, we define the space $H_{L,0}^\alpha(I)$ as the closure of ${}_0C^\infty(I)$ with respect to the norm $\|\theta\|_{H_L^\alpha(I)} := \left(\|\theta\|^2_{L^2(I)} + |\theta|^2_{H_L^\alpha(I)}\right)^{1/2}$, with $|\theta|_{H_L^\alpha(I)} := \|{}_0D_t^\alpha\theta\|_{L^2(I)}$.

Definition 3.2. For $\alpha > 0$, we define the space

$$H_R^\alpha(I) := \left\{\theta \in L^2(I); {}_tD_T^\alpha \theta \in L^2(I)\right\}$$

Furthermore, we define the space $H_{R,0}^\alpha(I)$ as the closure of ${}_0C^\infty(I)$ with respect to the norm $\|\theta\|_{H_R^\alpha(I)} := \left(\|\theta\|_{L^2(I)}^2 + |\theta|_{H_R^\alpha(I)}^2\right)^{1/2}$, with $|\theta|_{H_L^\alpha(I)} := \|{}_tD_T^\alpha \theta\|_{L^2(I)}$

Definition 3.3. For $\alpha > 0$ and $\alpha \neq n - \frac{1}{2}, n \in \mathbb{N}$, we define the space

$$H_S^\alpha(I) := \left\{\theta \in L^2(I); {}_0D_t^\alpha \theta \in L^2(I) \text{ and } {}_tD_T^\alpha \theta \in L^2(I)\right\}$$

Furthermore, we define the space $H_{S,0}^\alpha(I)$ as the closure of ${}_0C^\infty(I)$ with respect to the following norm $\|u\|_{H_S^\alpha(I)} := \left(\|\theta\|_{L^2(I)}^2 + \left|({}_0D_t^\alpha \theta, {}_tD_T^\alpha \theta)_{L^2(I)}\right|\right)^{1/2}$.

Definition 3.4. For $\alpha > 0$ and $\alpha \neq n - \frac{1}{2}, n \in \mathbb{N}$, we define the fractional Sobolev space $H^\alpha(I)$ as

$$H^\alpha(I) := \left\{\theta \in L^2(I) | |\omega|^\alpha \mathcal{F}(\tilde{\theta}) \in L^2(\mathbb{R})\right\}$$

where $\tilde{\theta}$ denotes an extension of θ by zero outside $I \subset \mathbb{R}$, and $\mathcal{F}$ denotes the Fourier transform. The space $H^\gamma(I)$ is equipped with the norm

$$\|\theta\|_{\alpha,I} := \left\| |\omega|^\gamma \mathcal{F}(\tilde{\theta}) \right\|_{0,\mathbb{R}}$$

We also define

$${}_0H^\alpha(I) := \left\{\theta \in H^\alpha(I) \mid \exists \theta_n \in {}_0C^\infty(I) \text{ such that } \lim_{n\to\infty} \|\theta_n - \theta\|_{\alpha,I} = 0\right\}.$$

Lemma 3.5 ([59]). . *Let $\alpha > 0$ with $\alpha \neq n - \frac{1}{2}$ for all $n \in \mathbb{N}$. Then the fractional derivative spaces $H_{L,0}^\alpha(I), H_{R,0}^\alpha(I), H_{S,0}^\alpha(I)$, and ${}_0H^\gamma(I)$ are equal, with equivalent norms.*

Lemma 3.6 ([34]). . *Let $0 < \alpha < 1$, then for $\theta \in H^\alpha(I)$, and $\vartheta \in H^{\frac{\alpha}{2}}(I)$ the following identity holds:*

$$({}_0\partial_t^\alpha \theta, \psi)_{0,I} = \left({}_0D_t^{\frac{\alpha}{2}} \theta, {}_tD_T^{\frac{\alpha}{2}} \psi\right)_{0,I} - \left(\frac{\theta(0)t^{-\alpha}}{\Gamma(1-\alpha)}, \psi\right)_{0,I}$$

Due to the presence of the singular potential term, the standard Sobolev spaces fail to provide an appropriate functional framework. Consequently, it becomes necessary to work within specially adapted functional spaces that account for the singularity. For a fixed real number $\mu \leq \frac{1}{4}$, let us introduce the following functional space:

$$H_0^{1,\mu}(\Lambda) := \left\{ u \in L^2(\Lambda) \cap H^1_{\text{loc}}((0,1]) \mid u(0) = u(1) = 0, \int_0^1 \left(u_x^2 - \mu \frac{u^2}{x^2} \right) dx < +\infty \right\}$$

The initial condition $u(.,0) = u_0$

is prescribed in the classical sense, which is compatible with the Caputo derivative. It should be noted that $H_0^{1,\mu}(\Lambda)$ is a Hilbert space obtained as the closure of $\mathcal{C}_0^\infty(\Lambda)$ with respect to the weighted norm

$$\|u\|_\mu := \left(\int_0^1 \left(u_x^2 - \mu \frac{u^2}{x^2} \right) dx \right)^{1/2}, \quad \forall z \in H_0^1(\Lambda)$$

In the sub-critical case when $\mu < \mu^* = \frac{1}{4}$, the Hardy inequality (1.5) ensures $\|\cdot\|_\mu$ and $\|\cdot\|_{H_0^1(0,1)}$, are equivalent norms, therefore, $H_0^{1,\mu}(\Lambda) = H_0^1(\Lambda)$. On the other hand, in the critical case $\mu = \mu^*$, it has been proved (see [**?**]) that this equivalence no longer holds, and the space $H_0^{1,\mu}(\Lambda)$ is strictly larger than $H_0^1(\Lambda)$. Next, we recall a fundamental compact embedding result (see [**?**]).

Theorem 3.7. *Let $\mu \leq \frac{1}{4}$.*
Then the embedding $H_0^{1,\mu}(\Lambda) \hookrightarrow L^2(\Lambda)$ is compact.

3.2.2 Variational formulation

In this subsection, we focus on establishing the existence of a weak solution to problem (1.1). To this end, we derive the corresponding weak formulation by making use of the preceding lemmas.

Let us denote $\Lambda := (0,1)$ and $\Omega = \Lambda \times I$. Assume that B is a Banach space defined over Λ, endowed with the norm $\|\cdot\|_B$. For $1 \leq q < \infty$, we define the Bochner-Lebesgue space

$$L^q(I;B) := \left\{ \theta : I \to B \mid \int_I \|\theta(t)\|_B^q dt < \infty \right\}$$

equipped with the norm

$$\|\theta\|_{L^q(I;B)} := \left(\int_I \|\theta(t)\|_B^q dt \right)^{1/q}$$

In the particular case where $B = L^2(\Lambda)$, it follows immediately that $L^2(I;B) = L^2(\Omega)$. Next, for any $\alpha > 0$, we define the fractional Sobolev space

$$\mathbf{H}^{\alpha}(I;B) := \left\{\theta \in L^2(I;B) \mid \|\theta(\cdot,t)\|_B \in H^{\alpha}(I) \text{ for all } t \in I\right\},$$

and similarly,

$$_0\mathbf{H}^{\alpha}(I;B) := \left\{\theta \in L^2(I;B) \mid \|\theta(\cdot,t)\| \in_0 H^{\alpha}(I) \text{ for all } t \in I\right\}.$$

These spaces are equipped with the norm

$$\|\theta\|_{\mathbf{H}^{\alpha}(I;B)} := \|\|\theta(\cdot,t)\|_B\|_{\alpha,I}.$$

Finally, we introduce a suitable functional space, which provides the appropriate framework to handle simultaneously the time-fractional derivative and the spatial singularity. Let us define the following Banach space

$$\mathbf{B}^{\alpha}_{\mu}(\Omega) := {}_0\mathbf{H}^{\alpha}\left(I; L^2(\Lambda)\right) \cap L^2\left(I; H^{1,\mu}_0(\Lambda)\right),$$

equipped with the norm

$$\|\theta\|^2_{\alpha,\mu} := \|\theta\|^2_{\mathbf{H}^{\alpha}(I;L^2(\Lambda))} + \|\theta\|^2_{L^2\left(I;H^{1,\mu}_0(\Lambda)\right)}$$

Within this framework, the weak formulation of the forward problem is stated as follows: find $\theta \in \mathbf{B}^{\frac{\alpha}{2}}_{\mu}(\Omega)$ such that

$$\mathcal{A}(\theta,\vartheta) = \mathcal{F}(\vartheta), \quad \forall \vartheta \in \mathbf{B}^{\alpha}_{\mu}(\Omega) \tag{2.1}$$

where the bilinear form $\mathcal{A}(\cdot,\cdot)$ and the linear functional $\mathcal{F}(\cdot)$ are given by

$$\mathcal{A}(\theta,\vartheta) := \left({}_0D^{\frac{\alpha}{2}}_t\theta, {}_tD^{\frac{\alpha}{2}}_T\vartheta\right)_{0,\Omega} + (\nabla\theta,\nabla\vartheta)_{0,\Omega} + \left(\frac{\mu}{x^2}\theta,\vartheta\right)_{0,\Omega}$$

and

$$\mathcal{F}(\vartheta) := \left(F + \frac{\theta_0 t^{-\alpha}}{\Gamma(1-\alpha)}, \vartheta\right)_{0,\Omega}$$

A key step in the analysis is to verify the coercivity and continuity of the bilinear form $\mathcal{A}(\cdot,\cdot)$ on the space $\mathbf{B}^{\alpha}_{\mu}(\Omega)$, as stated in the next lemma.

Lemma 3.8. *Let $0 < \alpha < 1$. The bilinear form $\mathcal{A}(\cdot,\cdot)$ is coercive and continuous on $\mathbf{B}^{\frac{\alpha}{2}}_{\mu}(\Omega)$, that is, there exist constants $\kappa_1 > 0$ and $\kappa_2 > 0$ such that for any $\theta,\vartheta \in \mathbf{B}^{\frac{\alpha}{2}}_{\mu}(\Omega)$, the following estimates hold:*

$$\mathcal{A}(\theta,\theta) \geq \kappa_1\|\theta\|^2_{\frac{\alpha}{2},\mu}, \quad |\mathcal{A}(\theta,\vartheta)| \leq \kappa_2\|\theta\|_{\frac{\alpha}{2},\mu}\|\vartheta\|_{\frac{\alpha}{2},\mu}. \tag{2.2}$$

Proof. We begin with the coercivity estimate. Recalling the definition of the bilinear form $\mathcal{A}(\cdot,\cdot)$, one has

$$\mathcal{A}(\theta,\theta) = \left({}_0D_t^{\frac{\alpha}{2}}\theta, {}_tD_T^{\frac{\alpha}{2}}\theta\right)_{0,\Omega} + \|\theta\|^2_{L^2\left(I;H_0^{1,\mu}(\Lambda)\right)}$$

By virtue of [[25], Proposition 2.5.], we have

$$\left({}_0D_t^{\frac{\alpha}{2}}\theta, {}_tD_T^{\frac{\alpha}{2}}\theta\right)_{0,\Omega} \geq \cos\left(\frac{\pi\alpha}{2}\right)\left\|{}_0D_t^{\frac{\alpha}{2}}\theta\right\|^2_{0,\Omega}.$$

Consequently, we arrive at

$$\mathcal{A}(\theta,\theta) \geq \kappa_1\|\theta\|^2_{\frac{\alpha}{2},\mu}, \quad \text{with} \quad \kappa_1 = \frac{1}{2}\min\left\{C_1\cos\left(\frac{\pi\alpha}{2}\right), 1\right\}$$

where $C_1 > 0$ arises from the equivalence of norms provided by lemma 3.2.1 This establishes the coercivity of $\mathcal{A}(\cdot,\cdot)$. We now turn to the continuity $\mathcal{A}(\cdot,\cdot)$. For arbitrary $\theta,\vartheta \in \mathbf{B}^{\alpha}_{\mu}(\Omega)$, we readily obtain by the Cauchy-Schwartz inequality

$$\begin{aligned}|\mathcal{A}(\theta,\vartheta)| &\leq \left\|0D_t^{\frac{\alpha}{2}}\theta\right\|_{0,\Omega}\left\|{}_tD_T^{\frac{\alpha}{2}}\vartheta\right\|_{0,\Omega} + \|\theta\|_{L^2\left(I;H_0^{1,\mu}(\Lambda)\right)}\|\vartheta\|_{L^2\left(I;H_0^{1,\mu}(\Lambda)\right)} \\ &\leq C_2\|\theta\|_{\mathbf{H}^{\frac{\alpha}{2}}(I,L^2(\Lambda))}\|\vartheta\|_{\mathbf{H}^{\frac{\alpha}{2}}(I,L^2(\Lambda))} + \|\theta\|_{L^2\left(I;H_0^{1,\mu}(\Lambda)\right)}\|\vartheta\|_{L^2\left(I;H_0^{1,\mu}.(\Lambda)\right)}\end{aligned}$$

Using the Hölder and Poincaré inequalities

$$|\mathcal{A}(\theta,\vartheta)| \leq \kappa_2\|\theta\|_{\frac{\alpha}{2},\mu}\|\vartheta\|_{\frac{\alpha}{2},\mu}$$

Hence, the bilinear form $\mathcal{A}(\cdot,\cdot)$ is continuous on $\mathbf{B}^{\frac{\alpha}{2}}_{\mu}(\Omega)$.
We now state a theorem that ensures the well-posedness of the weak formulation. (2.1). □

Theorem 3.9. *Let $0 < \alpha < 1$ and $f \in L^2(\Omega)$. Then, the weak formulation of problem (2.1) admits a unique solution $\theta \in \mathbf{B}^{\frac{\alpha}{2}}_{\mu}(\Omega)$. Moreover, there exists a constant $\kappa_3 > 0$, depending only on α, T, p, and Ω, such that the following estimate holds:*

$$\|\theta\|_{\frac{\alpha}{2},\mu} \leq \kappa_3\left(\|\theta_0\|_{L^2(\Lambda)}\left\|t^{-\alpha}\right\|_{L^q(I)} + \|F\|_{L^2(\Omega)}\right)$$

Proof. . The well-posedness of problem (2.20) follows from the classical Lax-Milgram theorem. Notice that the continuity and coercivity of the bilinear form $\mathcal{A}(\cdot,\cdot)$ are ensured by Lemma 3.2.4 It therefore remains to verify the continuity of the linear form $\mathcal{F}(\cdot)$. Applying the Cauchy-Schwarz inequality in $L^2(\Omega)$ to obtain

$$|\mathcal{F}(\vartheta)| \leq \left\| F + \frac{\theta_0 t^{-\alpha}}{\Gamma(1-\alpha)} \right\|_{0,\Omega} \|\vartheta\|_{0,\Omega}$$

and since $\|\vartheta\|_{0,\Omega} \leq C\|\vartheta\|_{\frac{\alpha}{2},\mu}$ it follows that, $|\mathcal{F}(\vartheta)| \leq C\|\vartheta\|_{\frac{\alpha}{2},\mu}$, which shows that $\mathcal{F}$ is continuous on $\mathbf{B}_\mu^{\frac{\alpha}{2}}(\Omega)$. Therefore, combining the coercivity and continuity of $\mathcal{A}(\cdot,\cdot)$ with the continuity of $\mathcal{F}(\cdot)$, all assumptions of the LaxMilgram theorem are satisfied. It follows that problem admits a unique weak solution in $\mathbf{B}_\mu^{\frac{\alpha}{2}}(\Omega)$.

Before addressing the inverse problem, it is first necessary to have a sufficient regularity for the solution of the associated direct problem. In particular, the assumption $\theta \in \mathbf{B}_\mu^{\frac{\alpha}{2}}(\Omega)$ as in Theorem does not imply $\partial_t\theta \in L^2\left(0,T;L^2(\Lambda)\right)$, which is indispensable for proving the uniqueness of the inverse source problem. or $\mu < \mu^*$, let us define the operator $\mathcal{L}_\mu$ in $L^2(\Lambda)$ as follows

$$\left(\mathcal{L}_\mu\vartheta\right)(x) := -\Delta\vartheta(x) - \frac{\mu}{x^2}\vartheta(x), \quad x \in \Lambda$$

where $\mathcal{L}_\mu$ equipped with Dirichlet homogeneous boundary conditions, with its domain $D\left(\mathcal{L}_\mu\right) = H_0^{2,\mu}(\Lambda)$. it can readily be checked that $\mathcal{L}_\mu$ is densely-defined closed, self-adjoint operator, therefore the fractional power operator $\mathcal{L}_\mu^\sigma$ is welldefined for any $\sigma \in \mathbb{R}$. According to Theorem, the spectrum of $\mathcal{L}_\mu$ consists of entirely of a sequence of positive eigenvalues

$$0 < \lambda_1 < \lambda_2 < \cdots < \lambda_n < \cdots \to +\infty$$

Let $\varphi_n \in H_0^{2,\mu}(\Lambda)$ be the L^2-orthonormal eigenfunctions corresponding to λ_n, namely,

$$\mathcal{L}_\mu\varphi_n := -\Delta\varphi_n - \frac{\mu}{x^2}\varphi_n = \lambda_n\varphi_n, \quad \forall n \in \mathbb{N}$$

Next, we define the space $\mathcal{H}^\sigma(\Lambda)$ as follows

$$\mathcal{H}^\sigma(\Lambda) := \left\{ \vartheta \in L^2(\Lambda) \left| \sum_{n=1}^{\infty} \lambda_j^\sigma \right| \left(\vartheta,\varphi_n\right)_{0,\Lambda} \right|^2 < \infty \right\},$$

which is a Hilbert space with the norm

$$\|\vartheta\|_{\mathcal{H}^\sigma(\Lambda)}^2 := \sum_{n=1}^{\infty} \lambda_j^\sigma \left|\left(v,\varphi_n\right)_{0,\Lambda}\right|^2$$

Let us introduce the operators $\mathbf{E}(t)$ and $\overline{\mathbf{E}}(t)$ defined by, respectively

$$\mathbf{E}(t)\vartheta = \sum_{n=1}^{\infty} E_{\alpha}\left(-\lambda_n t^{\alpha}\right)\left(\vartheta, \varphi_n\right)\varphi_n$$

and

$$\overline{\mathbf{E}}(t)v = \sum_{n=1}^{\infty} t^{\alpha-1} E_{\alpha,\alpha}\left(-\lambda_n t^{\alpha}\right)\left(v, \varphi_n\right)\varphi_n$$

where $E_{\alpha,\beta}(z)$ is the Mittag-Leffler function (we refer the reader to [40] for a detailed discussion on Mittag-Leffler function and their properties) . Consequently, the solution representation of θ can be written as

$$\theta(t) = \mathbf{E}(t)\theta_0 + \int_0^t \overline{\mathbf{E}}(t-s)F(\cdot, s)ds \tag{2.3}$$

It follows from the identity $\frac{d}{dt}E_{\alpha,1}\left(-\lambda_n t^{\alpha}\right) = -\lambda_n t^{\alpha-1} E_{\alpha,\alpha}\left(-\lambda_n t^{\alpha}\right)$ that

$$\frac{d}{dt}\mathbf{E}(t)\theta(t) = \overline{\mathbf{E}}(t)\mathcal{L}_{\mu}\theta(t)$$

Next, we turn to state some stability estimates on the solution operator $\mathbf{E}(t)$ and $\overline{\mathbf{E}}(t)$. □

Lemma 3.10 ([30]). . *For the operators $\mathbf{E}(t)$ and $\overline{\mathbf{E}}(t)$ defined in [40] and [41], respectively, we have, for any $t > 0$,*

$$\|\mathbf{E}(t)v\|_{H^p(\Omega)} \leq Ct^{-\frac{q-p}{2}}\|v\|_{H^q(\Omega)} \tag{2.4}$$

and

$$\|\overline{\mathbf{E}}(t)v\|_{H^p(\Omega)} \leq Ct^{-1-\frac{q-p}{2}}\|v\|_{H^q(\Omega)}, \tag{2.5}$$

where $0 \leq q \leq 2$ and $q \leq p \leq q+2$. The constant $C > 0$ depends only on Ω, p, and q.

Lemma 3.11 ([30]). *Assume that $\alpha > 0, \mu > 0$, and let $\phi(t)$ be a non-negative, locally integrable function on $(0, T)$. Suppose that $v(t)$ is also non-negative and locally integrable on $(0, T)$ with*

$$v(t) \leq \phi(t) + \mu \int_0^t (t-s)^{\alpha-1} v(s)ds, \quad 0 < t < T$$

Then, we have

$$v(t) \leq \phi(t) + \mu \int_0^t (t-s)^{\alpha-1} E_{\alpha,\alpha}\left(\mu(s)^{\alpha}\right)\phi(s)ds, \quad 0 < t < T$$

The following theorem contains the regularity result of the weak solution.

Theorem 3.12. *Let $\theta_0 \in \mathcal{H}^2(\Lambda)$ and $F \in H^1\left(0,T;L^2(\Lambda)\right)$. Then the solution θ to problem (1.1) satisfies*

$$\theta \in C\left([0,T];\mathcal{H}^2(\Lambda)\right) \cap C^1\left((0,T];L^2(\Lambda)\right), \quad D_t^\alpha \theta \in C\left((0,T];L^2(\Lambda)\right).$$

Proof. From the solution representation (2.3), one can derive

$$\theta_t(t) = \partial_t\left(\mathbf{E}(t)\theta_0\right) + \partial_t\left(\int_0^t \overline{\mathbf{E}}(t-s)F(\cdot,s)ds\right) \tag{2.6}$$

$$= \overline{\mathbf{E}}(t)\left(-\mathcal{L}_\mu\theta_0 + F(0)\right) + \int_0^t \overline{\mathbf{E}}(s)F_t(\cdot,t-s)ds \tag{3.1}$$

From this result, we have

$$\begin{aligned}
\|\theta_t(t)\|_{L^2(\Lambda)} &\leq \left\|\overline{\mathbf{E}}(t)\left(-\mathcal{L}_\mu\theta_0 + F(0)\right)\right\|_{0,\Lambda} + \int_0^t \left\|\overline{\mathbf{E}}(s)F_t(\cdot,t-s)\right\|_{0,\Lambda} ds \\
&\leq Ct^{\alpha-1}\left\|-\mathcal{L}_\mu\theta_0 + F(0)\right\|_{0,\Lambda} + C\int_0^t s^{\alpha-1}\left\|F_t(\cdot,t-s)\right\|_{0,\Lambda} ds \\
&\leq Ct^{\alpha-1}\left(\|F(0)\|_{0,\Lambda} + \|\theta_0\|_{\mathcal{H}^2(\Lambda)}\right) + C\|F\|_{C^1([0,T];L^2(\Lambda))}\int_0^t s^{\alpha-1}ds \\
&\leq Ct^{\alpha-1}\left(\|F(0)\|_{0,\Lambda} + \|\theta_0\|_{\mathcal{H}^2(\Lambda)}\right) + C't^\alpha\|F\|_{C^1([0,T];L^2(\Lambda))}
\end{aligned}$$

from which, we deduce that

$$\|\theta_t(t)\|_{L^2(\Lambda)} \leq Ct^{\alpha-1} + C't^\alpha = \eta(t)$$

Since $t \mapsto \eta(t)$ is a finite and continuous function for any $t \in (0,T]$, it follows that $\theta \in C^1\left((0,T];L^2(\Lambda)\right)$. Consequently, we obtain $\|D_t^\alpha\theta(t)\|_{0,\Lambda} \leq \int_0^t (t-s)^{-\alpha}\|\theta_t(s)\|\, ds \leq \|\theta\|_{C^1((0,T];L^2(\Lambda))}\int_0^t (t-s)^{-\alpha}ds \leq CT^{-\alpha}$, which achieves the proof of the desired result. ☐

This formulation follows the optimal control strategy developed in Chapter 2 and extends it to the time-fractional setting.

3.3 Uniqueness for the Inverse Problem

Building on the weak formulation and well-posedness results established in the previous section, we now turn to the inverse problem. In particular, we formulate and prove a uniqueness theorem, showing that the available data determine the unknown quantity in a consistent and well-defined manner.

Theorem 3.13. *Assume that the assumptions of **Theorem** 3.12 hold. Moreover, assume that $q(t) \in C^1([0,T])$ satisfies*

$$q(t)q'(t) \geq 0, \quad |q(t)| \geq c_0 > 0, \quad \forall t \in [0,T]$$

Then, there exists at most one couple

$$(\theta, p) \in C\left([0,T], H_0^{1,\mu}(\Lambda)\right) \times L^2(0,T)$$

solution of the inverse problem (IP).

Proof. Let (θ_1, p_1) and (θ_2, p_2) be two pairs of functions that solve (1.1) and satisfy (1.4). Define the differences $\theta := \theta_1 - \theta_2$, and $p := p_1 - p_2$. Then θ satisfies the homogeneous problem:

$$\begin{cases} \partial_t^\alpha \theta(x,t) - \Delta\theta(x,t) - \frac{\mu}{x^2}\theta(x,t) = p(x)q(t), & (x,t) \in \Omega \\ \theta(x,0) = 0, \quad x \in \Lambda, \\ \theta(0,t) = \theta(1,t) = 0, \quad t \in (0,T], \end{cases} \tag{3.1}$$

together with the terminal measurement

$$\theta(x,T) = 0, \quad x \in \bar{\Lambda} \tag{3.2}$$

Without loss of generality we consider the first case, that is, $q(t) \geq c_0 > 0$ and $q'(t) \geq 0$, for all $t \in [0,T]$. Hence, we can define $Q(t) := 1/q(t)$, which is an absolutely continuous function that satisfies $Q(t) > 0$ for all $t \in [0,T]$ and $Q \in L^\infty(0,T)$.

Now, let $\varepsilon > 0$ be fixed, and multiply the differential equation in (3.1) by the test function $Q(t)\partial_t\theta(x,t)$, integrate over Λ and then over (ε, T), we obtain

$$\int_\varepsilon^T Q(t)\left(\partial_t^\alpha \theta(t), \partial_t\theta(t)\right)_{0,\Lambda} dt \int_\varepsilon^T Q(t)\left(\nabla\theta(t), \nabla\partial_t\theta(t)\right)_{0,\Lambda} dt -$$
$$\int_\varepsilon^T Q(t)\left(\frac{\mu}{x^2}\theta(t), \partial_t\theta(t)\right)_{0,\Lambda} dt = \int_\varepsilon^T \left(p, \partial_t\theta(t)\right)_{0,\Lambda} dt \tag{3.3}$$

First, for the right-hand side of the above identity we have

$$\int_{\varepsilon}^{T} (p(x), \partial_t\theta(x,t))_{0,\Lambda}\, dt = (p(x), \theta(T) - \theta(\varepsilon))_{0,\Lambda} = -(p, \theta(\varepsilon))_{0,\Lambda} \tag{3.4}$$

Concerning the spatial terms, observe that

$$\int_{\varepsilon}^{T} Q(t)\,(\nabla\theta(t), \partial_t\nabla\theta(t))_{0,\Lambda}\, dt - \int_{\varepsilon}^{T} Q(t)\left(\frac{\mu}{x^2}\theta(t), \partial_t\theta(t)\right)_{0,\Lambda} dt =$$
$$\frac{1}{2}\int_{\varepsilon}^{T} Q(t)\partial_t\|\nabla\theta(t)\|_{0,\Lambda}^2 dt - \frac{1}{2}\int_{\varepsilon}^{T} Q(t)\partial_t|\theta(t)|_{\mu}^2 dt = \frac{1}{2}\int_{\varepsilon}^{T} Q(t)\partial_t\|\theta(t)\|_{\mu}^2 dt$$

Integrating by parts in time over $[\varepsilon, T]$ gives

$$\int_{\varepsilon}^{T} Q(t)\partial_t\|\theta(t)\|_{\mu}^2 dt = Q(T)\|\theta(T)\|_{\mu}^2 - Q(\varepsilon)\|\theta(\varepsilon)\|_{\mu}^2 - \int_{\varepsilon}^{T} Q'(t)\|\theta(t)\|_{\mu}^2 dt$$

Using $\theta(T) = 0$ and $Q' \leq 0$ yields

$$\int_{\varepsilon}^{T} Q(t)\partial_t\|\theta(t)\|_{\mu}^2 dt \geq -Q(\varepsilon)\|\theta(\varepsilon)\|_{\mu}^2 \tag{3.5}$$

We introduce the kerne $\omega^{\alpha}(t) = \frac{t^{-\alpha}}{\Gamma(1-\alpha)}$ for $t > 0$, then the Caputo derivative ${}_0\partial_t^{\alpha}\theta$ can then be expressed as the convolution $(\omega^{\alpha} * \partial_t\theta)(t)$ for $t > 0$. Now, let us set

$$a(t) := \left((\omega^{\alpha} * \partial_t\theta)(t), \partial_t\theta(t)\right)_{0,\Lambda}, \quad \text{and} \quad A(t) = \int_{\varepsilon}^{t} a(s)ds, \quad t \in [\varepsilon, T]$$

Since ω^{α} is positive-definite so $a(t) \geq 0$ for all $t \in [\varepsilon, T]$, and consequently $A(\cdot)$ is non-decreasing and finite on $[\varepsilon, T]$. Now, performing an integration by parts yields

$$\int_{\varepsilon}^{T} Q(t)a(t)dt = Q(T)A(T) - Q(\varepsilon)A(\varepsilon) - \int_{\varepsilon}^{T} Q'(t)A(t)dt$$

Keeping in mind that by definition $A(\varepsilon) = 0$ and $Q' \leq 0$ while $A(t) \geq 0$, we obtain

$$\int_{\varepsilon}^{T} Q(t)a(t)dt \geq Q(T)A(T) = Q(T)\int_{\varepsilon}^{T} a(s)ds \tag{3.6}$$

Combining the results (3.4), (3.5) and (3.6) with (3.3) yields

$$Q(T)\int_{\varepsilon}^{T} a(t)dt \leq |(p,\theta(\varepsilon))| + \frac{1}{2}Q(\varepsilon)\|\theta(\varepsilon)\|_{\mu}^{2}$$

Notice that $\theta(\varepsilon) \to 0$ in $H^{1,\mu}(\Lambda)$ as $\varepsilon \to 0$, therefore, the terms on the righthand side of the above inequality tend to 0 . Consequently, if follows that

$$\int_{0}^{T} a(t)dt = \lim_{\varepsilon\downarrow 0}\int_{\varepsilon}^{T} a(t)dt = 0$$

In view of $a(t) \geq 0$ a.e., therefore $a(t) = 0$ for a.e. $t \in (0,T)$, which implies $\partial_t\theta(\cdot,t) = 0$ a.e. on $(0,T)$ as an $L^2(\Lambda)$-valued function. Thus $\partial_t\theta(x,t) = 0$ for almost every $(x,t) \in \Lambda \times (0,T)$. Given $\theta(\cdot,0) = 0$, we conclude that $\theta \equiv 0$ on Ω. This in turn implies that $p = 0$.

The same argument applies with the sign changes required when $q(t) < 0$ and $q'(t) \leq 0$ on $[0,T]$. $\square$

Inversion algorithm and implementations

Let us consider the operator $\mathcal{A} : L^2(\Lambda) \to L^2(\Lambda)$, defined as

$$\mathcal{A}(p) := \theta[p](\cdot,T), \quad p \in L^2(\Lambda),$$

which associates to each source term $p(x)$ the final state $\theta[p](\cdot,T)$, where $\theta[p]$ denotes the unique weak solution to Problem (1.1) corresponding to the source term $p(x)$. By means of the operator $\mathcal{A}$, the inverse problem can be recast as an operator equation, namely,

$$\text{Find } p \in L^2(\Lambda), \text{ such that } : \mathcal{A}(p) = \omega_{obs} \tag{4.1}$$

where $\omega_{\text{obs}} \in L^2(\Lambda)$ represents the final state observation, corresponding to measurement condition (1.4).

Theorem 3.14. *The operator $\mathcal{A} : L^2(\Lambda) \longrightarrow L^2(\Lambda)$ is continuous.*

Proof. Let $p_1, p_2 \in L^2(\Lambda)$ and let $\theta_1 = \theta[p_1], \theta_2 = \theta[p_2]$ be the corresponding solutions of the forward problem. The difference $\theta = \theta_1 - \theta_2$ satisfies:

$$\begin{cases} \partial_t^{\alpha}\theta - \Delta\theta - \frac{\mu}{x^2}\theta = (p_1 - p_2)\, q(t), & (x,t) \in \Omega, \\ \theta(x,0) = 0, & x \in \Lambda, \\ \theta(0,t) = \theta(1,t) = 0, & t \in (0,T]. \end{cases}$$

Using the weak formulation from the paper, we have the energy estimate from Theorem 2,

$$\|\theta\|_{B_{\mu}^{\frac{\alpha}{2}}(\Omega)} \leq C \left\|\left(p_1 - p_2\right) q\right\|_{L^2(\Omega)} \leq C\|q\|_{L^{\infty}(0,T)} \left\|p_1 - p_2\right\|_{L^2(\Lambda)}$$

By the trace theorem for fractional Sobolev spaces, there exists a constant $C_T > 0$ such that

$$\|\theta(\cdot, T)\|_{H^1_{0,\mu}(\Lambda)} \leq C_T\|\theta\|_{L^2\left(I; H^1_{0,\mu}(\Lambda)\right)} \leq C_T\|\theta\|_{B_{\mu}^{\frac{\alpha}{2}}(\Omega)}$$

Combining the above estimates yields

$$\left\|\mathcal{A}\left(p_1\right) - \mathcal{A}\left(p_2\right)\right\|_{H^1_{0,\mu}(\Lambda)} = \|\theta(\cdot, T)\|_{H^1_{0,\mu}(\Lambda)} \leq C \left\|p_1 - p_2\right\|_{L^2(\Lambda)}$$

This shows that $\mathcal{A}$ is Lipschitz continuous, hence bounded. □

Theorem 3.15. *The operator $\mathcal{A} : L^2(\Lambda) \longrightarrow L^2(\Lambda)$ is compact.*

Proof. Let $(p_n)_{n\in\mathbb{N}}$ be a bounded sequence in $L^2(\Lambda)$. Therefore, by continuity of the operator $\mathcal{A}$ it follows that $\left(\mathcal{A}\left(p_n\right)\right)_{n\in\mathbb{N}}$ is uniformly bounded in $H_0^{1,\mu}(\Lambda)$. By the compact embedding $H_0^{1,\mu}(\Lambda) \hookrightarrow L^2(\Lambda)$ there exists a subsequence $\left(\mathcal{A}\left(p_{n_k}\right)\right)_{k\in\mathbb{N}}$ that converges strongly in $L^2(\Lambda)$. Therefore the image under $\mathcal{A}$ of every bounded sequence in $L^2(\Lambda)$ has a strongly convergent subsequence in $L^2(\Lambda)$, which is the definition of compactness. Hence $\mathcal{A} : L^2(\Lambda) \to L^2(\Lambda)$ is compact. Since the operator $\mathcal{A}$ is compact, thus the operator equation (4.1) represents an ill-posed inverse problem in the sense of Hadamard; that is, the solution, if it exists, does not depend continuously on the data. Therefore, it becomes necessary to employ regularization techniques to obtain stable approximate solutions that can be used in numerical computations. Among the most widely used methods in this context is the Tikhonov regularization method.

Accordingly, we define the associated Tikhonov functional by

$$\begin{aligned}\mathcal{J}_{\lambda}(p) &:= \frac{1}{2}\left\|\mathcal{A}(p) - \omega^{\delta}_{obs}\right\|^2_{L^2(\Lambda)} + \frac{\lambda}{2}\|p\|^2_{L^2(\Lambda)} \\ &= \frac{1}{2}\int_0^1 \left|\theta[p](x, T) - \omega^{\delta}_{obs}(x)\right|^2 dx + \frac{\lambda}{2}\int_0^1 |p(x)|^2 dx\end{aligned}$$

where $\lambda > 0$ is the regularization parameter and $\omega^{\delta}_{\text{obs}}$ is the noisy observation of ω satisfying

$$\left\|\omega_{\text{obs}}-\omega_{\text{obs}}^{\delta}\right\|_{L^2(\Lambda)} \leq \delta$$

for some sufficiently small $\delta > 0$. Accordingly, the inverse source problem is reformulated as the following variational minimization problem: find $p_\lambda^* \in L^2(\Lambda)$ such that

$$(\mathrm{P}_{\text{opt}}) \quad \begin{cases} \text{Find} : \quad p^* \in L^2(\Omega) \\ \mathcal{J}_\lambda(p^*) = \min_{p\in L^2(\Lambda)} \mathcal{J}_\lambda(p) \end{cases} \tag{4.2}$$

It is well known that problem (P_{opt}) admits a unique minimizer p_λ^δ, referred to as the Tikhonov regularized solution. Moreover, with a suitable choice of the regularization parameter $\lambda = \lambda(\delta)$, one can ensure that p_λ^δ converges to the exact solution p^* under a suitable choice of λ. Indeed, the regularization parameter λ is chosen to ensure the condition $\lim_{\lambda\to 0} \frac{\delta}{\sqrt{\lambda}} = 0$ is met, as recommended in [40]. Thus, the parameter λ can be taken to be $\lambda = 10^{-2}\delta^{4/5}$.

In this paper, we employ the Conjugate Gradient Method to find the minimizer of functional $\mathcal{J}_\lambda$. The key step for doing so lies in computing its gradient of $\mathcal{J}_\lambda$, which is stated in the next theorem. The presence of the fractional derivative leads to increased computational cost due to the memory term. □

Theorem 3.16. *Let $\theta[p]$ be the unique weak solution of the problem (1.1), and let $\omega^\delta \in L^2(0,1)$ be a noisy observation of $\theta(\cdot,T)$. Then, the functional $\mathcal{J}_\lambda : L^2(0,1) \to \mathbb{R}$ is Fréchet differentiable, and its gradient is given by:*

$$\nabla\mathcal{J}_\lambda(p)(x) = \int_0^T q(t)\psi(x,t)dt + \lambda p(x)$$

where $\psi = \psi[p]$ is the solution of the following adjoint problem:

$$\begin{cases} t\partial_T^\alpha\psi(x,t) - \Delta\psi(x,t) - \frac{\mu}{x^2}\psi(x,t) = 0, \quad (x,t) \in \Omega_T \\ \psi(x,T) = \theta[p](x,T) - \omega_{obs}^\delta(x), \quad x \in \Lambda \\ \psi(0,t) = \psi(1,t) = 0, \quad t \in (0,T) \end{cases}$$

Let p^k denote the k-th approximation of the exact source p. Define

$$p^{k+1} = p^k + \zeta_k d^k, \quad k = 0,1,2,\ldots, \tag{4.3}$$

where $p^0 \in L^2(0,1)$ is an initial guess, d^k is a descent direction, and $\zeta_k > 0$ is the step size. The descent direction d^k is updated following the classical Polak-Ribiere formulation Fletcher-Reeves

$$d^k = \begin{cases} -\nabla \mathcal{J}_\lambda \left(p^0\right), & \text{if } k = 0 \\ -\nabla \mathcal{J}_\lambda \left(p^k\right) + \alpha_k d^{k-1}, & \text{if } k \geq 1 \end{cases} \tag{4.4}$$

with the conjugacy coefficient α_k given by:

$$\alpha_k = \frac{\left\|\nabla \mathcal{J}_\lambda \left(p^k\right)\right\|^2_{L^2(0,1)}}{\left\|\nabla \mathcal{J}_\lambda \left(p^{k-1}\right)\right\|^2_{L^2(0,1)}}, \quad \alpha_0 = 0 \tag{4.5}$$

To compute the optimal step size ζ_k, we exploit the quadratic structure of the Tikhonov functional and impose the condition

$$\frac{\partial}{\partial \zeta} \mathcal{J}_\lambda \left(p^k + \zeta d^k\right) = 0$$

which yields the explicit expression:

$$\zeta_k = \frac{\int_0^1 \left(\theta\left[p^k\right](x,T) - \omega^\delta_{obs}(x)\right) \theta\left[d^k\right](x,T)dx + \lambda \int_0^1 p^k(x) d^k(x) dx}{\int_0^1 \left|\theta\left[d^k\right](x,T)\right|^2 dx + \lambda \int_0^1 \left|d^k(x)\right|^2 dx} \tag{4.6}$$

Here, $\theta\left[p^k\right]$ and $\theta\left[d^k\right]$ denote the solutions of the forward problem corresponding to the source terms p^k and d^k, respectively. The descent direction d^k is thus interpreted as a perturbation direction in the space of admissible source functions.

We now summarize the main steps of the Conjugate Gradient Method (CGM) employed to reconstruct the unknown source function $p(x)$ by minimizing the Tikhonov functional $\mathcal{J}_\lambda(p)$ defined above.

Algorithm 4 Conjugate Gradient Algorithm for Source Reconstruction

Initialization: Choose initial guess $p^0 \in L^2(0,1)$, set $k = 0$
Compute initial descent direction: $d^0 = -\nabla \mathcal{J}_\lambda(p^0)$
repeat
    Compute step size ζ_k using equation (4.6)
    Update approximation: $p^{k+1} = p^k + \zeta_k d^k$
    Evaluate gradient $\nabla \mathcal{J}_\lambda(p^{k+1})$
    Compute conjugacy coefficient α_{k+1} using equation (4.5)
    Update descent direction:

$$d^{k+1} = -\nabla \mathcal{J}_\lambda(p^{k+1}) + \alpha_{k+1} d^k$$

    Increment $k \leftarrow k + 1$
until stopping criterion is satisfied
Output: p^k as the reconstructed source function

3.4 Numerical experiments

In this section, we address the numerical reconstruction of the unknown spatial source term $p(x)$, utilizing the final measurement data ω^δ which is contaminated with noise, namely,

$$\omega^\delta_{obs}(x) = \omega_{obs}(x) + \delta \times \omega_{obs}(x) \cdot (2 \cdot \text{rand}(-1,1) - 1), \quad x \in (0,1),$$

where $\text{rand}(-1,1)$ denotes a uniformly distributed random variable in $(-1,1)$. The noise level is quantified by

$$\delta = \left\| \omega^\delta_{obs} - \omega_{obs} \right\|_{L^2(0,1)}$$

To assess the fidelity of the reconstructed source, we define the relative reconstruction error as

$$\mathcal{E}_k = \frac{\left\| p^{[k]} - p_{\text{true}} \right\|_{L^2(0,1)}}{\left\| p_{\text{true}} \right\|_{L^2(0,1)}},$$

where $p^{[k]}$ is the approximation obtained after k iterations. The residual error at the k-th iteration is given by

$$\mathcal{R}_k = \left\| u^{[k]}(x,T) - \omega^\delta_{obs} \right\|_{L^2(0,1)}$$

For the stopping rule, we employ the discrepancy principle, selecting the final iteration index K such that

$$\mathcal{R}_k \leq \tau\delta < \mathcal{R}_{k-1},$$

where $\tau > 1$ is a parameter typically set to $\tau = 1.01$. In the absence of noise ($\delta = 0$), the number of iterations is fixed at $k = 100$.

Example 3.17. Let the exact solution for the problem (1.1) be $\theta(x,t) = t^2 \sin(\pi x)$, then the source term to be reconstructed is given as $p(x) = \sin(\pi x)$, and the other parameters are obtained from the exact solution, that is,

$$w_{obs}(x) = T^2 \sin(\pi x), \quad q(t) = \frac{2t^{2-\alpha}}{\Gamma(3-\alpha)}, \quad f(x,t) = \left(\pi^2 - \frac{\mu}{x^2}\right) t^2 \sin(\pi x).$$

In this first example, we test the numerical performance of the proposed schema in recovering a smooth source term. First, we investigate the impact of the singular parameter μ on the inversion process. Figure 1 presents the sensibility of the numerical reconstruction to the value of μ. Panel (a) compares the exact and recovered profiles for $\mu = 0.05; 0.21; 0.39$. Panel (b) shows the pointwise difference between the exact and recovers source term. It is noticeable that the parameter μ measurably affects source reconstruction, as μ approaches the Hardy critical value $\mu^* = \frac{1}{4}$, the singular potential $\frac{\mu}{x^2}$ intensifies near $x = 0$, the forward operator spectral properties change, and the inverse problem becomes progressively more ill-conditioned, producing larger localized errors.

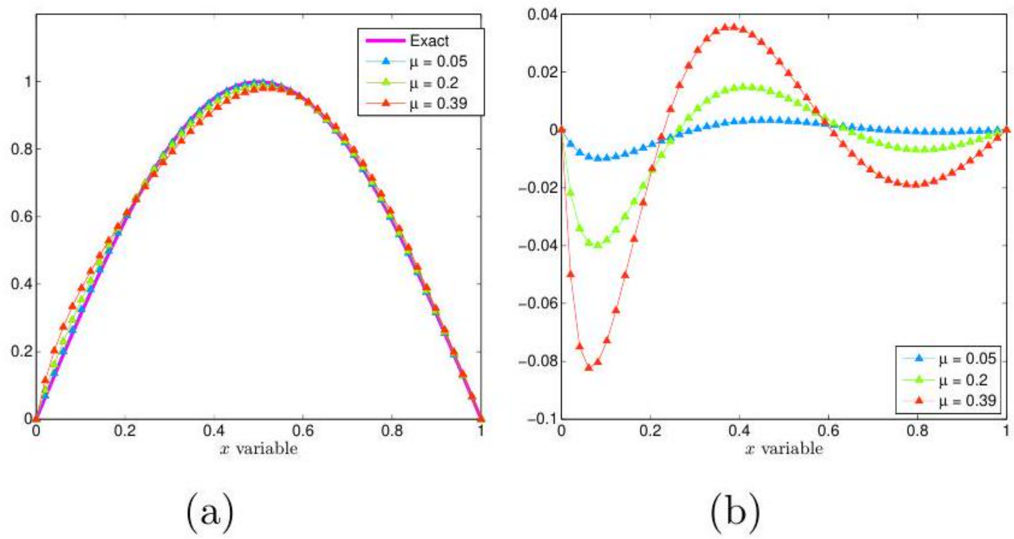

Figure 1. Sensibility of numerical reconstruction to μ in Example 1: (a) Profile of reconstructed solutions (b) Pointwise difference

Figure 2 depicts the profiles of the recovered source term corresponding to $\alpha = 0.3, 0.5, 0.8$. As α increases the relative error decreases which can be attributed to memory effect of the fractional derivative.

Table 1. Relative error $\mathcal{E}_k$ for Example 1 for different α and noise levels δ

	$\delta = 0$	$\delta = 0.01$	$\delta = 0.05$	$\delta = 0.1$
$\alpha = 0.3$	0.0235	0.0476	0.0784	0.0952
$\alpha = 0.5$	0.0221	0.0419	0.0611	0.0761
$\alpha = 0.8$	0.0202	0.0395	0.0583	0.0687

Figure 3 illustrates the results for the numerical reconstruction with different noise levels $\delta \in \{0; 0.01; 0.05; 0.1\}$ and fractional order $\alpha = 0.5$ and singular parameter $\mu = 0.2$. From Figure 2-(C), reconstructions still capture the main

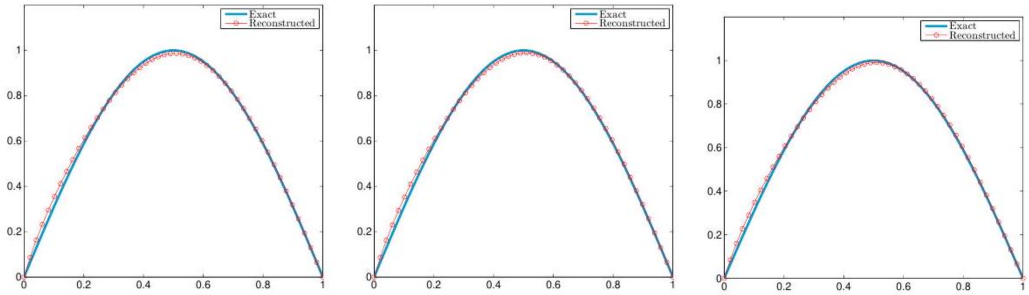

$\alpha = 0.3$ $\alpha = 0.5$ $\alpha = 0.8$

Figure 2. Exact and reconstructed solution for Example 1 for $\mu = 0.2$ different fractional order

profile even in the presence of noise. However, according to the reported results in Table (1) the noise level is not negligible and leads to larger final errors, for example, the relative error rises from $0.0235(\alpha = 0.3$ and $\delta = 0)$ to 0.0952 ($\alpha = 0.3$ and $\delta = 0.1$). Consequently, stronger regularization or edge-preserving priors are recommended for higher noise levels.

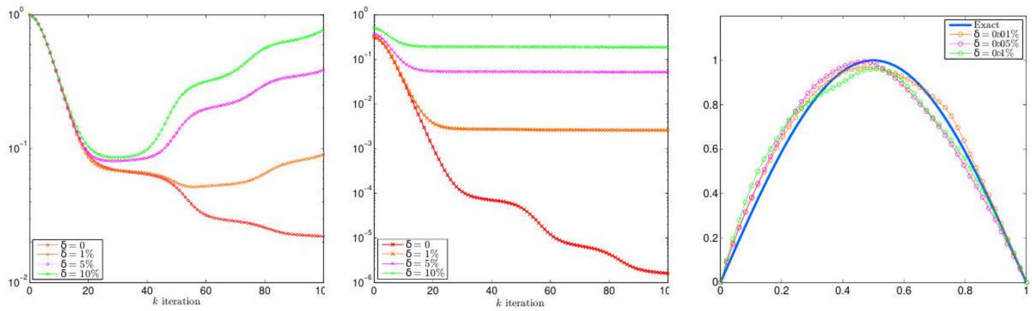

Error $\mathcal{E}_k$ Residual $\mathcal{R}_k$ Reconstructed solutions

Figure 3. Numerical reconstruction results for Example 1 with $\mu = 0.2, \alpha = 0.5$ and different noise levels

Example 3.18. In this example, we test the performance of the inversion algorithm in reconstructing a non-smooth source term given by

$$p(x) = \begin{cases} 1, & x \in \left[0, \frac{1}{2}\right[\cup \left]\frac{3}{4}, 1\right], \\ 2, & x \in \left[\frac{1}{2}, \frac{3}{4}\right], \\ 0, & \text{otherwise} . \end{cases}$$

The analytic expression of the exact solution is unknown, therefore, the final measurement data $\theta(\cdot, T)$ is simulated by solving the forward problem.

Table 2 presents the relative reconstruction errors $\mathcal{E}_k$ for Example 2, corresponding to the non-smooth target function. As expected, the errors increase with the noise level δ for all fractional orders α, reflecting the sensitivity of the inverse reconstruction to measurement perturbations. Moreover, for a fixed noise level, the reconstruction error decreases as α increases. This behavior is consistent with the fact that larger values of α yield models that are closer to the classical parabolic case, which are numerically more stable and less illposed. Compared with the smooth case, the errors are roughly twice as large, which is natural since the non-smooth profile involves sharp gradients that are more difficult to capture under regularization. Nevertheless, the error growth remains moderate, confirming the robustness of the proposed method with respect to data noise.

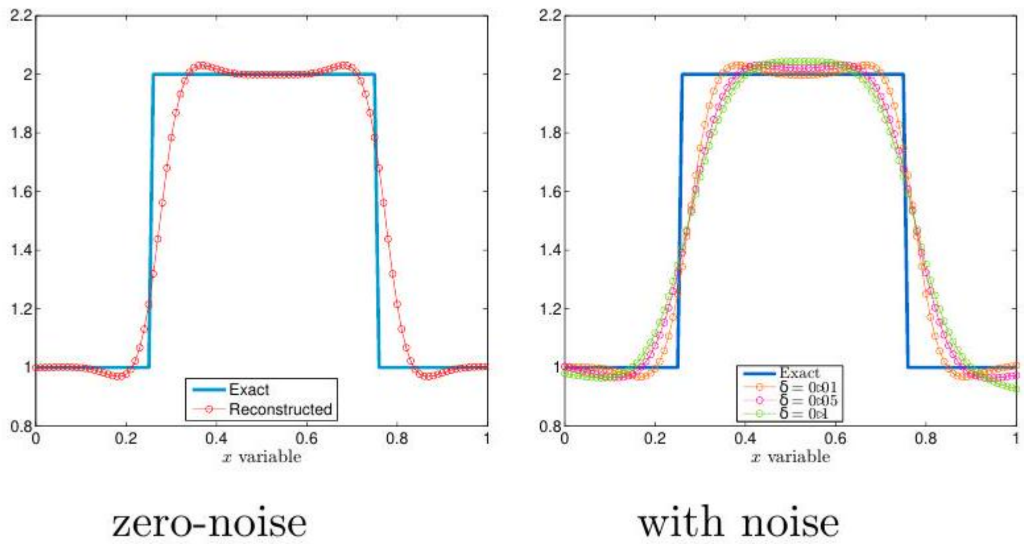

Figure 4. Numerical reconstruction results for Example 2 with different noise levels

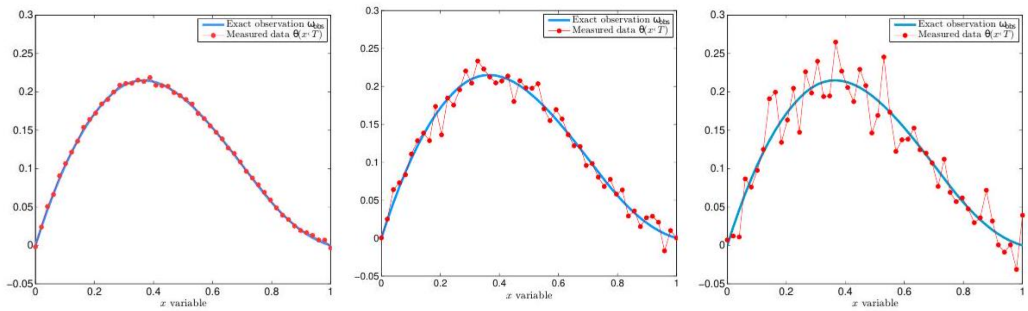

$\delta = 0.01$ $\delta = 0.05$ $\delta = 0.1$

Figure 5. Profile of measurement data under different noise levels

Table 2. Predicted relative error $\mathcal{E}_k$ for Example 2 (non-smooth case).

δ	0	0.01	0.05	0.10
$\alpha = 0.3$	0.0987	0.1064	0.1495	0.1891
$\alpha = 0.5$	0.0928	0.1000	0.1293	0.1738
$\alpha = 0.8$	0.0849	0.0915	0.1207	0.1610

Chapter 4

Shifted Carleman Inequalities for Singular Parabolic Operators

4.1 Introduction and motivation

This part looks into Carleman inequalities connected with parabolic equations where an inverse–square singular potential acts together with a variable diffusion coefficient. These inequalities have long stood at the core of how one studies observability and controllability, besides their use in several inverse problems involving parabolic models.

When a singular potential enters the picture, the standard Carleman arguments lose their direct applicability. The singular term interacts strongly with the elliptic operator and produces extra analytical strain, both in maintaining coercivity and in handling localisation near the critical region.

More concretely, one takes a parabolic operator written as

$$\mathcal{L}u := \partial_t u - \nabla\cdot\big(p(x)\nabla u\big) - \frac{\mu}{|x|^2}u,$$

with $p(x)$ a positive diffusion coefficient, while $\mu \geq 0$ marks the intensity of the inverse–square potential. The point $x = 0$ introduces a singular behaviour that forces one to work with special weighted tools rather than the usual schemes.

The chapter's aim is to build a Carleman setting that fits this singular configuration and to bring out the main analytical mechanisms which form the base of the estimate. well, such groundwork is meant to support later studies on observability inequalities and related inverse problems.

4.2 Setting of the problem and Hardy framework

Let Ω be a bounded domain in $\mathbb{R}^N$ ($N \geq 3$) with smooth boundary containing the origin, and take $T > 0$. Define

$$Q := \Omega \times (0,T), \qquad \Sigma := \partial\Omega \times (0,T).$$

The diffusion coefficient $p \in C^2(\overline{\Omega})$ is assumed to obey the uniform ellipticity bounds

$$0 < p_1 \leq p(x) \leq p_2 \quad \text{for all } x \in \overline{\Omega}.$$

We focus on the singular parabolic model

$$\begin{cases} \partial_t u - \nabla\cdot\big(p(x)\nabla u\big) - \dfrac{\mu}{|x|^2} u = g & \text{in } Q, \\ u = 0 & \text{on } \Sigma. \end{cases} \tag{4.1}$$

Because the inverse–square potential stands at the critical level under scaling, its treatment calls upon Hardy's inequality. For every $v \in H_0^1(\Omega)$,

$$\mu^* \int_\Omega \frac{|v|^2}{|x|^2}\, dx \leq \int_\Omega |\nabla v|^2\, dx, \qquad \mu^* := \frac{(N-2)^2}{4}.$$

All along this chapter we remain inside the subcritical range

$$0 \leq \mu < \frac{p_1}{p_2}\, \mu^*, \tag{4.2}$$

which makes it possible for the diffusion term to dominate the singular potential when one handles the weighted estimates. some lines may seem a bit rough, but that was the style of early drafts.

4.3 Choice of the Carleman weight

A careful design of the weight function lies at the heart of Carleman's method, the more so when a singular potential appears.

4.3.1 Spatial profile

A spatial function $k : \Omega \to \mathbb{R}$ is taken to meet

- $k \in C^2(\Omega \setminus \{0\})$,

- $k(x)$ reproduces the singular feature near $x = 0$,
- $|\nabla k(x)|$ stays nonzero away from a small neighbourhood around the singularity.

Close to the origin, k follows a logarithmic pattern, matching the inverse–square structure of the potential. Set

$$\Phi(x) := e^{\lambda k(x)},$$

with $\lambda > 0$ taken large.

4.3.2 Time shift and space–time weight

Choose $t_0 \in (0, T)$ and $\beta > 0$, and define

$$\psi(x,t) := k(x) - \beta|t - t_0|^2, \qquad \varphi(x,t) := e^{\lambda\psi(x,t)}.$$

This time shift brings the weight to focus inside the time interval, a property of value in observability and inverse problem tasks. For $s > 0$, define finally

$$\sigma(x,t) := s\varphi(x,t).$$

4.4 Conjugation and operator decomposition

4.4.1 Weighted unknown

Take u to be a smooth enough solution of (4.1). Introduce the weighted function

$$z(x,t) := e^{-\sigma(x,t)}u(x,t), \qquad u(x,t) = e^{\sigma(x,t)}z(x,t).$$

The related conjugated operator is written as

$$\mathcal{P}z := e^{-\sigma}\mathcal{L}(e^{\sigma}z).$$

A short though direct calculation gives

$$\begin{aligned}\mathcal{P}z = \partial_t z - \nabla\cdot(p\nabla z) + 2p\,\nabla\sigma\cdot\nabla z - (\partial_t\sigma)z - p(\Delta\sigma)z \\ - p|\nabla\sigma|^2 z - \nabla p\cdot\nabla\sigma\, z - \frac{\mu}{|x|^2}z.\end{aligned}$$

4.4.2 Symmetric and antisymmetric parts

We break $\mathcal{P}$ into two components,

$$\mathcal{P}z = Sz + Az,$$

where

$$Sz := -\nabla\cdot(p\nabla z) - p(\Delta\sigma)z - \nabla p\cdot\nabla\sigma\, z - \frac{\mu}{|x|^2}z,$$

and

$$Az := \partial_t z + 2p\,\nabla\sigma\cdot\nabla z - (\partial_t\sigma)z - p|\nabla\sigma|^2 z.$$

Such a splitting turns out to be central, for it isolates the singular term and lets one handle it through Hardy-type arguments inside the interaction expression. (sometimes I still re-check that step; it's easy to slip on signs.)

4.5 Fundamental identity and interaction term

Squaring the transformed equation and integrating across Q one finds

$$\int_Q |Sz + Az|^2 = \int_Q |Sz|^2 + \int_Q |Az|^2 + 2\int_Q (Sz)(Az) = \int_Q e^{-2\sigma}|g|^2.$$

The essential contribution lies within the mixed term

$$2\int_Q (Sz)(Az),$$

for it produces the coercive quantities that lie behind the Carleman estimate..

4.6 Partial estimates and analytical difficulties

Expanding $2\int_Q (Sz)(Az)$ in detail brings out several groups of terms: gradient parts, zero–order ones, singular fragments, and smaller remainders. The main positive expressions appear as

$$\int_Q s\lambda^2\varphi\,|\nabla z|^2, \qquad \int_Q s^3\lambda^4\varphi^3\,|z|^2.$$

The potential with $\frac{1}{|x|^2}$ gives rise to pieces like

$$\int_Q \frac{|z|^2}{|x|^2},$$

which remain manageable thanks to Hardy's inequality under the subcritical rule (4.2), provided s and λ are large enough.

Still, further weighted expressions containing time derivatives, for instance

$$\int_{\tilde{o}\times(0,T)} (\theta\Phi)^{-1} e^{-2s\sigma} |\partial_t z|^2,$$

need sharper Caccioppoli-type tools together with fine localisation work. Handling these inside the singular framework is rather delicate and stands among the chief technical burdens of the study, if anything.

4.7 Status of the Carleman analysis and ongoing work

The reasoning given in this part sets up a sound Carleman structure for the singular parabolic case. The choice of the weight, the decomposition of the operator, and the appearance of coercive terms are all worked out, leading already to partial Carleman inequalities.

Yet to reach a fully global estimate, one must still cope with some heavy weighted time-derivative terms and control the remaining parts. These difficulties stem naturally from the singular inverse-square character and are well recognised in earlier analyses.

Hence the material here should be read as an open piece of research. The analytical frame stands ready, the obstacles are sharply defined, and the completion of the final inequality remains under study with my supervisor. Finishing this task forms a key continuation beyond the present thesis work—perhaps the most demanding stretch of it.

General Conclusion

This thesis has centred on the study of inverse problems for singular and degenerate parabolic equations, approached through a blend of analytical reasoning and numerical experimentation. The guiding theme has been the recovery of spatially dependent source terms from partial data, in settings where ill-posedness and singular effects both exert a decisive influence...

In **Chapter 2**, an inverse source problem for a parabolic equation carrying an inverse-square potential was re-expressed as an optimal-control formulation. Under subcritical assumptions on the singular coefficient, we proved the well-posedness of the corresponding direct problem within weighted Sobolev spaces and showed the existence of an optimal solution.

By deriving first-order necessary optimality conditions, a stability bound was obtained, linking the reconstructed source to perturbations in the terminal observations.

A Landweber-type iterative procedure was then implemented to compute reconstructions numerically—confirming the theoretical expectations, and indicating the robustness of the approach.

Chapter 3 extended the investigation to time-fractional diffusion models with the same inverse-square feature. The inclusion of fractional time derivatives introduced strong non-local behaviour; this added both analytical and computational difficulty. Even so, we established uniqueness for the inverse source problem and proposed algorithms able to accommodate the combined effects of singularity and memory. The corresponding simulations revealed how the quality of the reconstruction depends on the fractional order, and on measurement noise, thereby clarifying practical limitations of the method.

Chapter 4 turned to the development of Carleman inequalities for singular parabolic operators. This section proved the most technically demanding, since classical Carleman arguments had to be reshaped to cope with the inverse-square term. After constructing suitable weight functions and conjugating the operator, we separated the resulting expression into symmetric and antisymmetric parts, then examined the interaction contributions between them. Partial Carleman-type estimates were secured, and the analytic pattern of the global inequality was laid out...

Achieving a complete Carleman estimate, however, still requires delicate control of weighted time-derivative terms and the use of Caccioppoli-type inequalities suited to singular weights and intersecting geometric zones. These operations are subtle, relying on careful localisation and a sensitive balance between the Carleman parameters; the remaining obstacles are intrinsic to the model and reflect the critical behaviour of the potential. The work therefore chooses to expose and analyse these obstacles rather than conceal them.

Overall, the thesis offers both firm results and an open framework. It contributes explicit findings on uniqueness, stability, and reconstruction for inverse problems driven by singular or fractional parabolic dynamics, while at the same time establishing the groundwork for further progress. Future directions include the completion of the Carleman analysis of Chapter 4, its possible extension to higher-dimensional or multipolar singularities, and the design of more efficient, noise-resistant numerical schemes.

The continuation of the Carleman study is already under way in collaboration with my supervisor. Given the intrinsic difficulty of the problem, this continuation forms a natural sequel to the present investigation and is expected to yield further analytical advances. In this sense, the present work should be regarded not as a final point, but as a structured step towards a deeper understanding of inverse problems for singular parabolic operators—and perhaps, a modest invitation to pursue what remains unresolved.

Bibliography

[1] Alabau-Boussouira, F. (2006). Controllability of cascade coupled systems of PDEs. *ESAIM: Control, Optimisation and Calculus of Variations*, **11**(3), 426–448.

[2] Allal, D., & Maniar, L. (2015). Null controllability of degenerate and singular parabolic equations. *Mathematical Control and Related Fields*, **5**(1), 1–23.

[3] Alziary, B., Azorero, J.P., & Peral, I. (1998). Hardy inequalities, potentials and Schrödinger operators in $\mathbb{R}^N$. *Journal of Mathematical Analysis and Applications*, **218**(2), 457–490.

[4] Apanapudor, J.S., Umukoro, J., Okwonu, F.Z., & Okposo, N. (2023). Optimal solution techniques for control problem of evolution equations. *The Scientific World Journal*, **2023**, Article ID 123456.

[5] Atifi, K., Boutaayamou, I., Ould Sidi, H., & Salhi, J. (2018). An inverse source problem for singular parabolic equations with interior degeneracy. *Abstract and Applied Analysis*, **2018**, 1–16.

[6] Azorero, J.G., & Peral, I. (1998). Hardy inequalities and some critical elliptic and parabolic problems. *Journal of Differential Equations*, **144**(2), 441–476.

[7] Baras, P., & Goldstein, J.A. (1984). The heat equation with a singular potential. *Transactions of the American Mathematical Society*, **284**(1), 121–139.

[8] Baras, P., & Goldstein, J.A. (1984). Remarks on the inverse square potential in quantum mechanics. *North-Holland Mathematics Studies*, **92**(C), 31.

[9] Bebernes, J., & Eberly, D. (2013). *Mathematical Problems from Combustion Theory* (Vol. 83). Springer Science & Business Media.

[10] Benabbes, F., Boussetila, N., & Lakhdari, A. (2024). The modified fractional-order quasi-reversibility method for a class of direct and inverse problems governed by time-fractional heat equations with involution perturbation. *Mathematical Methods in the Applied Sciences*, **47**(12), 9524–9555.

[11] Benabdallah, A., Cristofol, M., Gaitan, P., & Yamamoto, M. (2009). Inverse problem for a parabolic system with two components by measurements of one component. *Applicable Analysis*, **88**(5), 683–709.

[12] Berestycki, H., & Esteban, M.J. (1997). Existence and bifurcation of solutions for an elliptic degenerate problem. *Journal of Differential Equations*, **134**(1), 1–25.

[13] Bukhgeim, A.L., & Klibanov, M.V. (1981). Global uniqueness of a class of multidimensional inverse problems. *Soviet Mathematics Doklady*, **24**, 244–247.

[14] Cannarsa, P., Doubova, A., & Yamamoto, M. (2021). Inverse problem of reconstruction of degenerate diffusion coefficient in a parabolic equation. *Inverse Problems*, **37**(12), 125002.

[15] Coşkun, A.E. (2020). An inverse problem in estimating the time dependent source term and initial temperature simultaneously by the polynomial regression and conjugate gradient method. *Mathematical Methods in the Applied Sciences*, **43**(1), 45–62.

[16] De Castro, A.S. (2004). Bound states of the Dirac equation for a class of effective quadratic plus inversely quadratic potentials. *Annals of Physics*, **311**(1), 170–181.

[17] Colaco, M.J., Orlande, H.R.B., & Özisik, M.N. (2006). Comparison of different versions of the conjugate gradient method applied to inverse heat transfer problems. *Numerical Heat Transfer, Part B*, **49**, 389–406.

[18] Engl, H.W., Hanke, M., & Neubauer, A. (1996). *Regularization of Inverse Problems.* Springer, Mathematics and Its Applications, Vol. 375.

[19] Feng, X., Zhao, M., & Qian, Z. (2022). A Tikhonov regularization method for solving a backward time-space fractional diffusion problem. *Journal of Computational and Applied Mathematics*, **411**, 114236.

[20] Fletcher, R., & Reeves, C.M. (1964). Function minimization by conjugate gradients. *The Computer Journal*, **7**(2), 149–154.

[21] Gao, Y., & Yin, D. (2021). A full-stage creep model for rocks based on the variable-order fractional calculus. *Applied Mathematical Modelling*, **95**, 435–446.

[22] Giri, P.R., Gupta, K.S., Meljanac, S., & Samsarov, A. (2008). Electron capture and scaling anomaly in polar molecules. *Physics Letters A*, **372**(17), 2967–2970.

[23] Hestenes, M.R., & Stiefel, E. (1952). Methods of conjugate gradients for solving linear systems. *J. Res. Nat. Bur. Standards*, **49**, 409–436.

[24] Hilfer, R. (2000). *Applications of Fractional Calculus in Physics.* World Scientific.

[25] Huang, J.F., Nie, N.M., & Tang, Y.F. (2014). A second order finite difference spectral method for space fractional diffusion equations. *Science China Mathematics*, **57**(6), 1303–1317.

[26] Imanuvilov, O.Y., & Yamamoto, M. (1998). Lipschitz stability in inverse parabolic problems by the Carleman estimate. *Inverse Problems*, **14**(5), 1229–1245.

[27] Imanuvilov, O.Y., & Yamamoto, M. (2022). Inverse parabolic problems by Carleman estimates with data taken at initial or final time moments of observation. *Journal of Inverse and Ill-posed Problems*, **30**(3), 395–416.

[28] Jin, B., Lazarov, R., Liu, Y., & Zhou, Z. (2017). Numerical methods for time-fractional evolution equations with nonsmooth data: A concise overview. *Computers & Mathematics with Applications*, **73**, 1631–1644.

[29] Jin, B., & Rundell, W. (2015). A tutorial on inverse problems for anomalous diffusion processes. *Inverse Problems*, **31**(3), 035003.

[30] Kaltenbacher, B., & Rundell, W. (2019). On the identification of a nonlinear term in a reaction-diffusion equation. *Inverse Problems*, **35**(11), 115007.

[31] Khompysh, K., Huntul, M.J., Shazyndayeva, M.K., & Iqbal, M.K. (2024). An inverse problem for pseudoparabolic equation: existence, uniqueness, stability, and numerical analysis. *Mathematics*, **12**(3), Article 451.

[32] Kilbas, A.A., Koroleva, A.A., & Rogosin, S.V. (2013). Multi-parametric Mittag-Leffler functions and their extension. *Fractional Calculus and Applied Analysis*, **16**(2), 378–404.

[33] Lax, P.D. (2002). *Functional Analysis*. Wiley.

[34] Li, X., & Xu, C. (2009). A space-time spectral method for the time fractional diffusion equation. *SIAM Journal on Numerical Analysis*, **47**(3), 2108–2131.

[35] Lin, Y., & Xu, C. (2007). Finite difference/spectral approximations for the time-fractional diffusion equation. *Journal of Computational Physics*, **225**, 1533–1552.

[36] Magin, R. (2004). Fractional calculus in bioengineering, part 1. *Critical Reviews in Biomedical Engineering*, **32**(1).

[37] Mahdi, N., & Chettouh, A. (2024). Inverse problem for a time-fractional diffusion equation with singular potential. *Mathematical Methods in the Applied Sciences*, **47**(17), 12435–12458.

[38] Mainardi, F. (2022). *Fractional Calculus and Waves in Linear Viscoelasticity: An Introduction to Mathematical Models*. World Scientific.

[39] Metzler, R., & Klafter, J. (2000). The random walk's guide to anomalous diffusion: a fractional dynamics approach. *Physics Reports*, **339**(1), 1–77.

[40] Morozov, V.A. (2012). *Methods for Solving Incorrectly Posed Problems*. Springer Science & Business Media.

[41] Nouar, M., & Chattouh, A. (2024). On the source identification problem for a degenerate time-fractional diffusion equation. *Journal of Mathematical Analysis*, **15**(5).

[42] Nouar, M., & Chattouh, A. (2025). On recovering space-dependent source term in a degenerate nonlocal parabolic equation. *Journal of Mathematical Modeling*, **13**(4), 645–662.

[43] Özisik, M.N., & Orlande, H.R.B. (2000). *Inverse Heat Transfer: Fundamentals and Applications*. Taylor Francis.

[44] Podlubny, I. (1999). *Fractional Differential Equations*. Academic Press, Mathematics in Science and Engineering, Vol. 198.

[45] Qin, X. (2024). Carleman estimate and applications for a heat equation with multiple singularities. *Applicable Analysis*, **103**(1), 1–22.

[46] Srati, M., Oulmelk, A., Afraites, L., & Hadri, A. (2025). An inverse problem of identifying two coefficients in a time-fractional reaction diffusion system. *Discrete and Continuous Dynamical Systems-S*, **18**(1), 113–147.

[47] Tautenhahn, U. (1994). Optimality for ill-posed problems under general source conditions. *Numerical Functional Analysis and Optimization*, **15**, 567–582.

[48] Vancostenoble, J. (2011). Lipschitz stability in inverse source problems for singular parabolic equations. *Communications in Partial Differential Equations*, **36**(8), 1287–1317.

[49] Vázquez, J.L., & Zuazua, E. (2000). The Hardy inequality and the asymptotic behaviour of the heat equation with an inverse-square potential. *Journal of Functional Analysis*, **173**, 103–153.

[50] Wang, Z., Qiu, S., Yu, S., Wu, B., & Zhang, W. (2023). Exponential Tikhonov regularization method for solving an inverse source problem of time fractional diffusion equation. *J. Comput. Math*, **41**(2), 173–190.

[51] Wei, T., & Luo, Y. (2022). A generalized quasi-boundary value method for recovering a source in a fractional diffusion-wave equation. *Inverse Problems*, **38**(4), 045001.

[52] Wen, J., Liu, Z.X., Yue, C.W., & Wang, S.J. (2022). Landweber iteration method for simultaneous inversion of the source term and initial data in a time-fractional diffusion equation. *Journal of Applied Mathematics and Computing*, **68**(5), 3219–3250.

[53] Wen, J., & Yong-Ping Wang. (2023). The quasi-reversibility regularization method for backward problems of the time-fractional diffusion-wave equation. *Physica Scripta*, **98**(9), 095250.

[54] Yamamoto, M. (2009). Inverse problems for evolution equations. *World Scientific Lecture Notes in Mathematics*, **28**, 1–75.

[55] Yang, F., Fu, J.L., Fan, P., & Li, X.X. (2021). Fractional landweber iterative regularization method for identifying the unknown source of the time-fractional diffusion problem. *Acta Applicandae Mathematicae*, **175**(1), 13.

[56] Yang, L., Yu, J.N., Luo, G.W., & Deng, Z.C. (2012). Reconstruction of a space and time dependent heat source from finite measurement data. *International Journal of Heat and Mass Transfer*, **55**(23), 6573–6581.

[57] Zhang, M., Li, Q., & Liu, J. (2023). On stability and regularization for data-driven solution of parabolic inverse source problems. *Journal of Computational Physics*, **474**, 111769.

[58] Zhang, M., & Zhang, Z. (2023). Solving the inverse potential problem in the parabolic equation by the deep neural networks method. *Neural Computing and Applications*, **35**, 11255–11272.

[59] Zheng, M., Liu, F., Turner, I., & Anh, V. (2015). A novel high order space-time spectral method for the time fractional Fokker–Planck equation. *SIAM Journal on Scientific Computing*, **37**(2), A701–A724.